https://ntrs.nasa.gov/search.jsp?R=19850012595 2020-03-20T18:47:13+00:00Z

General Disclaimer

One or more of the Following Statements may affect this Document

- This document has been reproduced from the best copy furnished by the organizational source. It is being released in the interest of making available as much information as possible.

- This document may contain data, which exceeds the sheet parameters. It was furnished in this condition by the organizational source and is the best copy available.

- This document may contain tone-on-tone or color graphs, charts and/or pictures, which have been reproduced in black and white.

- This document is paginated as submitted by the original source.

- Portions of this document are not fully legible due to the historical nature of some of the material. However, it is the best reproduction available from the original submission.

Produced by the NASA Center for Aerospace Information (CASI)

NASA TECHNICAL MEMORANDUM NASA TM-77818

DETERMINATION OF THE MOBILITY PROFILE IN GaAs-MESFETs

W. Prost

(NASA-TM-77818) DETERMINATION OF THE MOBILITY PROFILE IN GaAs-MESFETS Thesis (National Aeronautics and Space Administration) 50 p HC A05/MF A01 CSCL 20L N85-20905

G3/76 Unclas 14483

Translation of "Bestimmung des Beweglichkeitsprofils in GaAs-MESFETs." THESIS. Duisberg University, West Germany, June 1983, pp. 1-120.

NATIONAL AERONAUTICS AND SPACE ADMINISTRATION
WASHINGTON, DC 20546 MARCH 1985

STANDARD TITLE PAGE

1. Report No. NASA TM-77818	2. Government Accession No.	3. Recipient's Catalog No.
4. Title and Subtitle DETERMINATION OF THE MOBILITY PROFILE IN GaAs-MESFETs		5. Report Date March 1985
		6. Performing Organization Code
7. Author(s) W. Prost		8. Performing Organization Report No.
		10. Work Unit No.
9. Performing Organization Name and Address The Corporate Word 1102 Arrott Building Pittsburgh, PA 15222		11. Contract or Grant No. NASW-4006
		13. Type of Report and Period Covered Translation
12. Sponsoring Agency Name and Address National Aeronautics and Space Administration Washington, D.C. 20546		14. Sponsoring Agency Code

15. Supplementary Notes

Translation of "Bestimmung des Beweglichkeitsprofils in GaAs-MESFETs", Thesis, Duisberg University, West Germany, June 1983, pp. 1-120.

16. Abstract

A process for measuring charge carrier mobility for gallium-arsenid metal semi-conductor-field effect transistors is described in an attempt to optimize the relationship between this factor and production. The physical basis for the process is outlined, as are features of the measuring room. The measuring technique is described and recommendations for setting measuring parameters are made.

17. Key Words (Selected by Author(s))	18. Distribution Statement Unlimited

19. Security Classif. (of this report)	20. Security Classif. (of this page)	21. No. of Pages	22. Price
Unclassified	Unclassified	90	

NASA-HQ

TABLE OF CONTENTS

1	Introduction	7
1.1	Motivation and Purpose	7
1.2	Magneto-transconductance-mobility-profiling	9
2	Physical basis	9
2.1	Mobility, transconductance	9
2.2	Physical basis of the measuring principle	12
2.2.1	Physical conductance reduction	14
2.2.2	Geometric conductance reduction	14
2.3	Application of physical phenomenon to the real structural elements	18
2.3.1	The GaAs-short channel-MESFET	18
2.3.2	The structural element as Hall-structure	19
2.3.3	Influence of magnetic fields on conductance	21
2.4	Influence of idealization	22
2.4.1	Finite geometry	23
2.4.2	Parasitic resistance	24
2.4.3	Idealized structure and summary observation of physical and geometric mistakes	30
3	Measuring room	32
3.1	Measuring principle	32
3.2	Measuring instruments and voltage supply	35
3.2.1	Lock-in-amplifier	35
3.2.2	Kiethley-digital multimeter	38
3.2.3	Voltage supply	38
3.2.4	Test circuit	39
3.3	Magnetic field-control loop	41
3.3.1	Magnetic field-control loop instruments	43
3.3.2	Magnetic field control	44
3.4	Measuring room automation	49
4	Measuring technique	52
4.1	Observation of errors	52
4.1.1	Sources of errors	52
4.1.2	Error sensitivity	53
4.1.3	Statistical procedures	57
4.1.3.1	Control of input data	58
4.1.3.2	Error compensation using "linear regression"	60
4.1.4	Drift phenomena	61

4.2 Technical boundaries of the measuring process 63

4.3 Setting recommendations of measuring parameters 65

5. Results 68

5.1 Diffused MESFETs 68
5.2 Epitaxial MESFETs 72
5.3 Hetero-MESFETs 75

6 Conclusion 76

Appendix: Program read-out 78

References 89

LIST OF FIGURES

No.	Content	Page
1.1.1	Optimum cycle of structural element production	7
1.1.2	Survey of procedures aimed at a locally resolved mobility profile	8
1.2.1	Schematic mobility profile	9
2.1.1	Output characteristic curve field of a MESFET	10
2.1.2	Output characteristic curve field in the starting range	11
2.2.1	Geometry of a Hall structure	13
2.2.2	Current and equipotential field curves of a semiconductor plate in a magnetic field with the side relation L/W=2,4 according to [2]	15
2.3.1	Schematic cross section of a MESFET	18
2.3.2	Tolerance of effective Hall structure	20
2.4.1	Geometric function for resistance increase of right-angled semiconductor plates	24
2.4.2	Replacement switch representation characterizing the drain-source current	25
2.4.3	Simplified representation of a replacement switch characterizing i_{ds}	25
2.4.4	Distribution of the error function f_b and its causes in the channel	29
2.4.5	Experimental confirmation of the evaluation equation	31
3.1.1	Flow diagram of the measuring cycle	33
3.1.2	Model of a measuring device	34
3.1.3	Technical realization of a measuring device	35
3.2.1	Application range of the lock-in amplifier	36
3.2.2	Comparison of reference and entrance voltage of the lock-in amplifier	36
3.2.3	Test circuit	39
3.2.4	Acceptable value range of the gate-source	40
3.2.5	The test circuit in the block circuit of the measuring device	41
3.3.1	Block circuit for digital magnetic field regulation	43
3.3.2	Magnetic field regulating circuit	44
3.3.3	Transfer function of instrument group A	46
3.3.4	Time plan of the magnetic field regulation	48
3.4.1	Structure of computer controlled measuring program	49
3.4.2	Entire block circuit of measuring room	51

4.1.1	Adjustment specification for the magnetic field on the basis of acceptable errors and average mobility	56
4.1.2	Error offset by line approximation	57
4.1.3	Transient process of a measuring value after changing the setting dimensions	58
4.1.4	Storage bank for k=4	59
4.1.5	Uncorrected drifts in measuring device	62
4.1.6	Corrected drifts of the measuring device	63
4.3.1	Estimation value of mobility of different tests	66
4.3.2	Calculable transconductance range in dependency of u_{gs} and S_E	67
5.1.1	III-49 Mobility profile	69
5.1.2	III-49 Line approximation	69
5.1.3	III-49 Tabulated mobility profile	70
5.1.4	III-78 Mobility profile	71
5.1.5	Data comparison for two diffused tests	71
5.2.1	I-208b Tabular mobility profile	73
5.2.2	I-208b Mobility profile	74
5.2.3	ALF 1003/1 Mobility profile	74
5.3.1	Structure of a hetero-MESFET	75
5.3.2	D-6-9a Mobility profile	76

DETERMINATION OF THE MOBILITY PROFILE IN GaAs-MESFETs

W. Prost

1 Introduction /1*

1.1 Motivation and Purpose

The Institute for Semiconductor Technology (HLT) at the University of Duisburg (West Germany) produces and investigates gallium-arsenide-metal-semiconductor-field effect-transistors (GaAs-MESFET). It is the goal of the Institute to optimize certain characteristics of the structural elements through directed influence on technology.

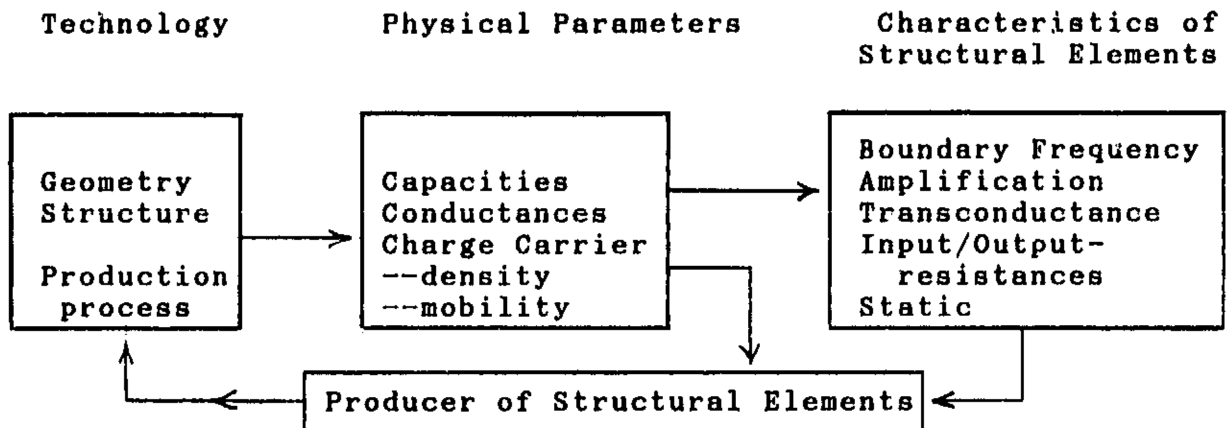

Fig. 1.1.1: Optimum cycle of structural element production

The producer of the structural elements observes the influence of technology on the physical parameters and on the finished /2 product. A change in structural element production aimed at optimization of the desired relationship requires full awareness of all available data. The interdependence of these quantities is so great and varied that conscious optimization is unthinkable without awareness of the physical parameters.

The object of this thesis is to supply producers of structural elements with a measuring process which incorporates one of these physical parameters, namely charge carrier mobility, and its local dispersion in the channel (mobility profile).

*Numbers in the margin indicate pagination in the original text.

It is already possible to determine charge carrier concentration, DC power characteristic curves, and microwave characteristics by means of measuring technology. The incorporation of the mobility profile, therefore, supplements the Institute's measuring technology.

Due to the reciprocal action of all data involved in the production process, it is advantageous to be able to measure the physical parameters on the structural element itself rather than on a special measuring structure (for example, Hall-Kreuz). Further, the measuring process should be nondestructive, so that the structural element is available for further measurements and can be characterized in detail. Both of these criteria led to the selection of the measuring procedure.

/3

No.	Methods	Locally resolved?	Destruction?	Special Measure Structure?	Literature
1	Chemical	indirect	yes	yes	[7]
2	Long-channel	indirect	no	yes	[5]
3	van der Pauw (diff.)	indirect	no	yes	[6]
4	Magneto-resistance	indirect	no	no	[4]
5	Magnetotrans-conductance	direct	no	no	[1]

Table 1.1.2: Survey of procedure aimed at a locally resolved mobility profile

We see from Table (1.1.2) that procedures 4 and 5 satisfy the aforementioned assumptions. The decided advantage of No. 5 lies in the fact that mobility $b(x_0)$ is measured in a very thin layer (δ=0,6-6 nm) at x_0, while all of the other procedures determine $b(x_0)$ as integral mobility over the still open channel of x_0 to $x=d_0$, the boundary of the semi-insulating material (SI).

For this reason, only procedure No. 5, MAGNETO-TRANSCONDUCTANCE-MOBILITY-PROFILING, is capable of definitely recognizing the extremely important boundary layer effects at the gate contact, as well as those on the boundary surface to the SI.

1.2 MAGNETO-TRANSCONDUCTANCE-MOBILITY-PROFILING /4

This concept identifies the measuring process which evaluates the change in transconductance in a magnetic field in order to determine charge carrier mobility in the channel. This procedure does not determine charge carrier mobility as a mean value over the entire density of the channel, but rather as a value on a defined position x_0.

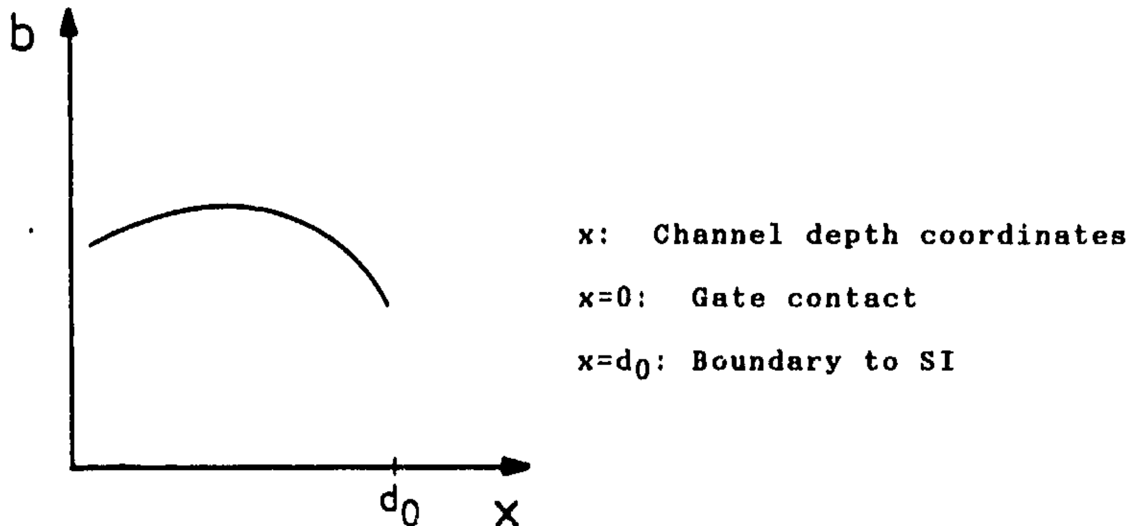

Fig. 1.2.1: Schematic mobility profile

The procedure is applicable to all normal MESFETs with a gate length in the range of 1 μm as used in microwave circuits.

2 Physical basis /5

2.1 Mobility, transconductance

If an external voltage U is applied to a semiconducting crystal, an electric field strength E occurs in the crystal and applies a force to the electrically charged particles.

$$\vec{F} = q \cdot \vec{E} \qquad (2.1.1)$$

If the charge carriers are not connected to the grid, this load leads to a movement of the charge carriers and also to a flow of current. Charge carriers do not move uniformly. They are disturbed in their movement by collisions with grid atoms and ionized atoms. By taking the mean, one arrives at the following relationship:

$$\vec{v} = \frac{qt_R}{m^*} \cdot \vec{E} \qquad (2.1.2)$$

$\vec{v}$: Drift speed
t_R : Relaxation time
m^* : Effective mass of the charge carrier

Drift speed is proportional to the electric field. The proportionality factor is called charge carrier mobility.

$$\frac{qt_R}{m^*} = b \qquad (2.1.3)$$

From equations (2.1.2) and (2.1.3) it follows that:

$$\vec{v} = b \cdot \vec{E} \qquad (2.1.4)$$

Ohmic law is applied to attain the relationship for the conductance of the crystal. /6

$$\vec{g} = \sigma \cdot \vec{E} = q \cdot n \cdot \vec{v} \qquad \text{(Ohm's law)}$$

$$\sigma = q \cdot n \cdot b \qquad (2.1.5)$$

$\vec{g}$: Electric current density
n : Charge carrier concentration
σ : Electric conductance

The relationship (2.1.2) is not valid for all high field strengths. Speed saturation occurs beginning at a defined field strength E_S.

$$v = v_{Sat} \qquad (2.1.6)$$

For all field strengths $E > E_S$ relationships (2.1.3) to (2.1.5) are no longer valid. This is of great importance in determining the measuring process, since it follows that charge carrier mobility can only be determined in the valid range of the ohmic law.

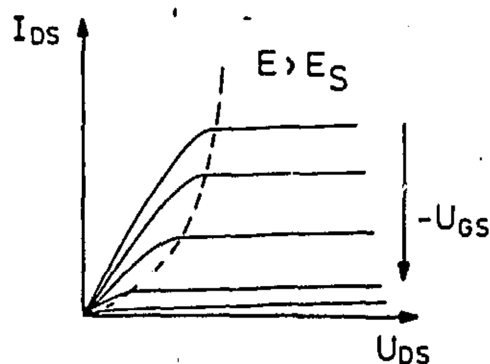

Fig. 2.1.1: Output characteristic curve field of a MESFET

The measurements must, for this reason, always be carried out at working points (U_{DS}, U_{GS}), which guarantee $E \ll E_S$. /7

The more uniform the crystal structure, the greater the mobility of the charge carrier in the crystal. Dislocations, discontinuities, and other grid disturbances impair the mobility of the charge carriers. Also the necessary doping of semiconductors is a disturbs the crystal grid and leads to a reduction of charge carrier mobility. For this reason a compromise has to be found between high current density resulting from high discontinuities and high mobility resulting from low discontinuity concentration.

The measuring procedure depends upon the transconductance of the magnetic field. For this reason, we shall now concentrate on the concept of transconductance.

$$S = \lim_{\Delta U_{GS} \to 0} \frac{\Delta I_{DS}}{\Delta U_{GS}} \qquad (2.1.7)$$

In the linear range of the characteristic curve field (saturation ranges no longer being considered) transconductance increases linearly with U_{DS}.

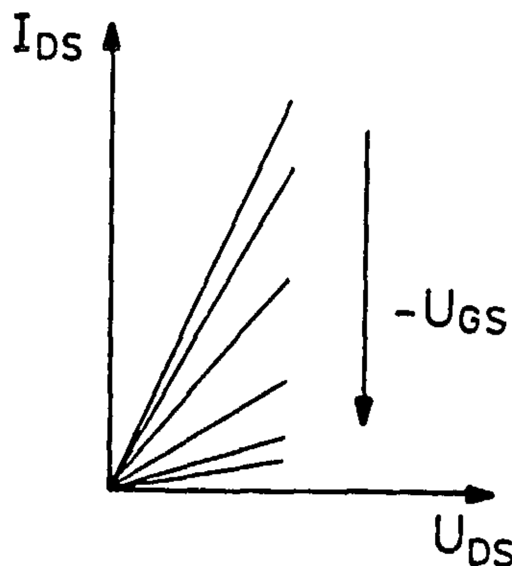

Fig. 2.1.2: Output characteristic curve field in the starting range

For each respective working point the transconductance characterizes the grid penetration factor contained in a change of the input quantity U_{GS} upon the output quantity I_{DS}. The transconductance of a MESFET is determined by gate capacity and current depth. In the linear range a relationship between /8

transconductance and electric conductivity can be obtained with the help of equation (2.1.7) and the ohmic law.

$$S = \sigma \cdot \lim_{\Delta U_{GS} \to 0} \frac{\Delta (E \cdot A)}{\Delta U_{GS}} \qquad (2.1.8)$$

E : Field strength in the channel
A : Cross section of the channel opened through U_{GS}

Transconductance is proportional to σ in the linear range.

2.2 Physical basis of the measuring principle

As already mentioned in Chapter (1.2), the measuring principle essentially consists of measurement of the tansconductance

-- with magnetic field
-- without magnetic field

In order to better understand the effects and the derivation of the algorithm, which, on the basis of these measurements, determines charge carrier mobility, we shall now investigate the influence of the magnetic field upon transconductance. Since equation (2.1.8) makes a proportionality between transconductance and electric conductivity evident, it suffices to describe the magnetic field dependency of σ.

In the electric and magnetic field a force F acts upon charge carriers in the crystal, which in practice is composed of an n-doped material or electrons:

$$\vec{F} = -e \cdot (\vec{E} + \vec{v} * \vec{B}) \qquad (2.2.1)$$ /9

e : Electric elementary load
B : Magnetic flow density

Under the influence of this force, the charge carriers drift away from their course, which would run parallel to the electric field if it weren't for the magnetic field. On the one side of the conducting crystal a relative charge carrier deficiency occurs, while on the other side a relative charge carrier excess comes into being. A potential difference occurs between the two sides, the "Hall-potential" U_H.

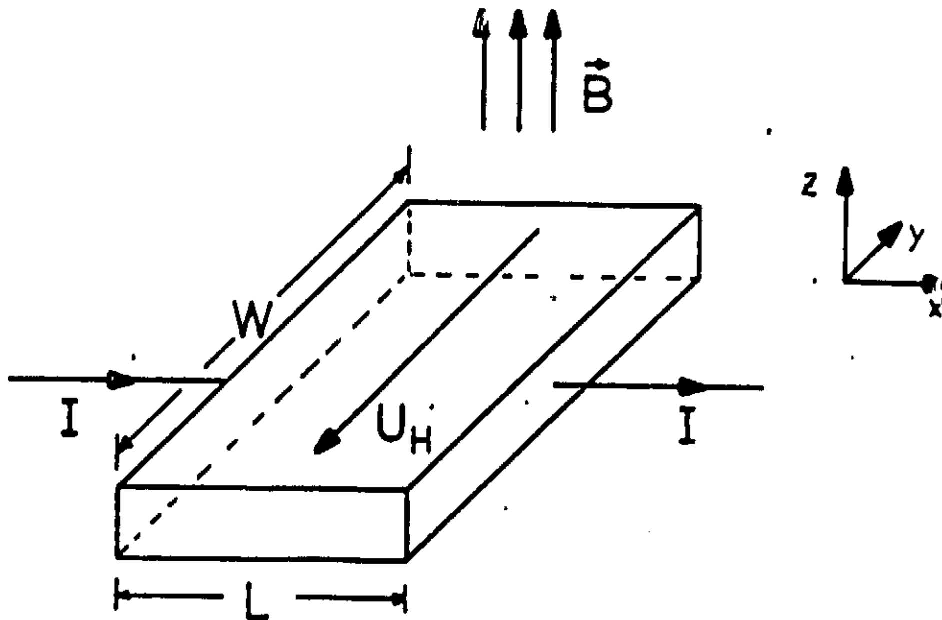

Fig. 2.2.1: Geometry of a Hall structure

The field strength E_y increases until it has compensated the Lorentz portion $\vec{v} \times \vec{B}$. Statically, no force acts upon the charge carriers in direction $\vec{e}_y$. They cross the semiconductor along the field curve of E_x, that is the shortest course. Along the current depth has changed in opposition to the situation B=0. It increases in direction $-\vec{e}_y$. No change in electric conductivity is to be expected. A reduction of conductance first occurs when the transient phenomenon is disturbed between Lorentz /10 portion $\vec{v} \times \vec{B}$ and E_y and the charge carrier no longer crosses the crystal by the shortest course. There are two causes for this:

-- the physical resistance effect $P(n, p, b_n, b_p)$
-- the geometric resistance effect $G_R(L/W, \Theta_H)$

$$\Theta_H \sphericalangle (\vec{E}, \vec{q}) \tag{2.2.2a}$$

E : Resulting field strength in the crystal
p : Concentration of positive charge carriers

With these assumptions a statement of electric conductivity is defined as a function of magnetic field dependency :

$$\sigma(B) = \frac{\sigma(0)}{G_R(L/W, \Theta_H) \cdot P(n, p, p, b_n, b_p)} \tag{2.2.2b}$$

2.2.1 Physical conductance reduction

In the case of a two-unit conductor, n and p are equal or of equal magnitude and a compensation of the Hall field strength occurs. Positive as well as negative charge carriers are displaced in the same direction by the force $q \cdot \vec{v} * \vec{B}$, so that on the sides charge carriers are simultaneously charged positively and/or negatively. Compensation occurs and the Hall field strength decreases. Since, however, the Lorentz force continues without decrease in strength to act upon the charge carriers the current lines become crooked. The path through the crystal becomes longer and electric conductivity decreases. /11

Aside from the concentrations n and p, the effect is still dependent upon the charge carrier mobility (p. [2]). For $n \gg p$, not enough p-charge carriers are available to cause a noticeable compensation. For doped semiconducter material it is, therefore, valid, that:

$$P(n \gg p) = 1 \qquad (2.2.3)$$

Accordingly, the physical resistance effect cannot be responsible for the decrease in transconductance of highly doped MESFETs in a magnetic field.

2.2.2 Geometric conductance reduction

Every real Hall structure has finite dimensions, which are defined here by

- L : Length in direction of control current
- W : Length in direction of the Hall potential which is formed

(see Fig. 2.2.1). Along W the Hall structure is metallically contacted, to facilitate better control current feed. Near this metallic contact:

$$E_y = 0$$

On ideally conductive materials, field curves of the electric field strength will always be perpendicular. This means, however, that no Hall field strength can develop there and that the current lines are therefore crooked. /12

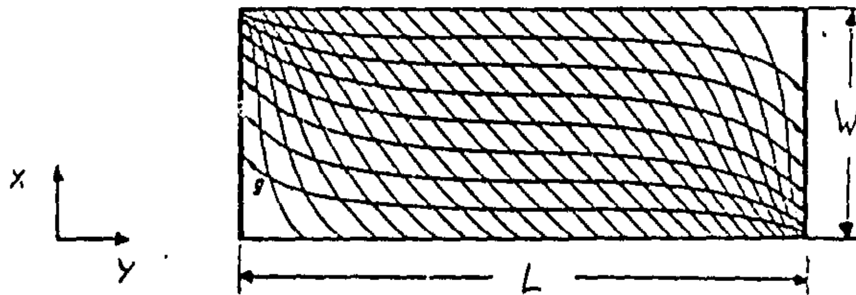

Fig. 2.2.2: Current and equipotential field curves of a semiconductor plate in a magnetic field with ratio L/W = 2.4 according to /2/.

Figure (2.2.2) clarifies how the Hall field strenght disappears and causes the current curves to become crooked at the contacts. In the middle of the Hall structure the Hall field strength is completely developed and the current curves run parallel to the applied electric field E_x.

In the case $L/W \rightarrow \infty$, the ranges with crooked current curves are relatively minimal and the effect can be ignored.

$$G_R \ (L/W \rightarrow \infty) = 1 \qquad (2.2.4a)$$

Actually in an actual short channel-MESFET the relationship is approximately:

$$L/W = 0.0023$$

For this reason we must consider the boundary case L/W = 0 more closely. In this case the transient phenomenon is completely destroyed and therefore

/13

$$G_R \ (L/W \rightarrow 0) = G_{R\ max} \qquad (2.2.4b)$$

The mathematics for the description of this process are quite involved. Here it will have to suffice to quote statements and results ([2] p. 74ff).

Generally, Maxwell equations with a problem set up according to Figure (2.2.2) are applied for universal L/W. Kuhrt and Lippmann find a solution through conforming illustrations:

$$G_R\left(\frac{L}{W}, \Theta_H\right) = \frac{W}{L} \cdot \frac{1}{\cos \Theta_H} \cdot \frac{Z_R}{N} \qquad (2.2.5a)$$

Z_R and N are integral expressions in accordance with:

$$Z_R = \int_0^\infty \frac{\cosh\left(2 \frac{\Theta_H}{\pi} \cdot v\right)}{\sqrt{\frac{4k}{(1+k)^2} + \sinh^2 v}} \, dv \qquad (2.2.5b)$$

$$V = \int_0^{\infty} \frac{\cosh(2 \frac{\Theta_H}{\pi} \cdot v)}{\sqrt{\left(\frac{1-k}{1+k}\right)^2 + \sinh^2 v}} \, dv \tag{2.2.5c}$$

$$L/W = \frac{K(\sqrt{1-k^2})}{2 \cdot K(k)} . \tag{2.2.5d}$$

$K(\mu)$ is the "complete elliptic integral". Equation (2.2.5) describes the geometric function G_R for universal L/W. For the application, however, we must consider the boundary case $G_R(L/W = 0)$.

The boundary value formation $L/W \rightarrow 0$ on the equation (2.2.5) applies the following geometric function in a simplified form:

$$G_R \;(L/W \;\; 0, \Theta_H) = 1 + \tan^2 \Theta_H \tag{2.2.6}$$

As the form of the equation (2.2.5) already suggests, the boundary value formation is not elementary, but rather requires complex calculations. Here, too, one should refer to literature /2/.

The equation (2.2.6), however, is a fairly manageable mathematical intermediate result. The variable Θ_H is nonetheless a disturbing factor. It still has to be replaced. For this purpose one uses the relation:

$$\tan \;_H = \sigma \;(B) \cdot R_H(B) \cdot B \tag{2.2.7}$$

This relationship is known from the theory of the Hall generators. For strongly doped semiconductor material in the exhausted range $R_H(B)$ becomes:

$$R_H = - \frac{1}{e \cdot N_D} \tag{2.2.8}$$

N_D : Doping level

Kuhrt and Lippmann report, that this is valid for magnetic flow densities up to 18 tesla ([2], p. 71). In equation (2.2.7) the physical conductance reduction is indicated with $\sigma = \sigma(B)$, which has already been excluded for highly doped materials in Chapter (2.2.1). With the universal definition equation of the conductivity for n-conducting material

$$\sigma = -e \cdot b \cdot N_D \tag{2.2.9}$$

and equation (2.2.8) equation (2.2.7) becomes:

$$\tan \Theta_H = b \cdot B \tag{2.2.10}$$

The mobility of the charge carriers can be calculated using /15 equations (2.2.8) and (2.2.9).

$$b = R_H \cdot \sigma \qquad (2.2.11)$$

It is particularly important here that the Hall constant R_H and electric conductivity are not functions of magnetic flow density. It follows that:

$$b \neq f(B) \qquad (2.2.12)$$

Equation (2.2.10) inserted into equation (2.2.6) results in:

$$G_R(L/W \rightarrow 0) = 1 + b^2 \cdot B^2$$

$$\sigma(B) = \frac{\sigma(0)}{1 + b^2 \cdot B^2} \qquad (2.2.14)$$

With respect to b, equation (2.2.14) can be solved thusly:

$$b = \frac{1}{B} \sqrt{\frac{\sigma(0)}{\sigma(B)} - 1} \qquad (2.2.15)$$

Since b is not a function of magnetic flow density, equation (2.2.15) can be considered a physically viable possibility for determining charge carrier mobility. Prerequisite to this application is the preservation of all idealizations which were made in attaining equation (2.2.15):

1. $n \gg p$

2. $L/W \rightarrow 0$

3. The field curves of the electric field strength are perpendicular to the contacts.
   $E_y = 0$

4. To solve the integral expression (2.2.5) a Taylor series /16 development of the course of an electron was used. Between two collisions with the grid the electron's course in the magnetic field describes a cycloid [2]. The following simplifications are therefore valid, if only a small part of the cycloid is traversed, so that the approximation using Taylor series developments is sufficiently precise. In the literature the following boundaries are cited:

   $b \cdot B \lesssim 1$ [4]
   $b \cdot B \ll 1$ [2]

2.3 Application of physical phenomena to real structural elements

/17

2.3.1 GaAs-short channel-MESFET

Let us now consider a schematic drawing of the function and the geometry of the structural element.

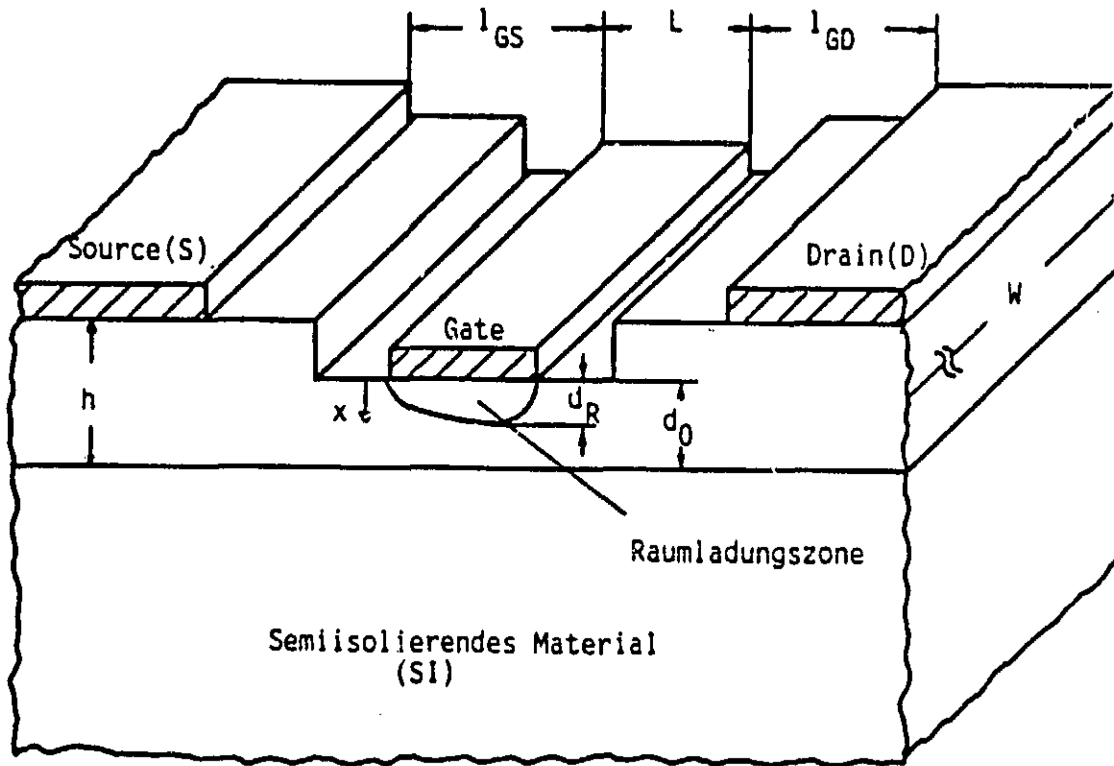

Fig. 2.3.1: Schematic cross section of a MESFET
(R) = space charge zone
(SI)= semi-insulation material

Typical geometric data are:

Gate length	$L = 0.7\ \mu m$
Gate width	$W = 300\ \mu m$
Gate-source distance	$l_{GS} = 2.5\ \mu m$
Gate-drain distance	$l_{GD} = 2.5\ \mu m$
Total channel density	$d_0 = 60$ to 300 nm
Passage area height	$h = 200$ to 400 nm

Source (S) and drain (D) are block-free ohmic contacts. /18
Gate (G) is a blocking metal-semiconductor control electrode. Current flows from the source to the drain and is directed by the gate electrode. To this end voltage U_{GS} is applied between the

gate and the source. This voltage determines the density of the space charge zone under the gate and with it the density of the open channel. It can vary between:

$$U_T \leq U_{GS} \leq U_{Bi}$$

U_T : the channel is constricted and the voltage applied between the drain and source cannot drive any current (except for a residual current) through the structural element.

U_{Bi} : the space charge zone is discharged. The channel is open from the gate contact to the SI, so that the channel resistance is minimal and the drain-source current I_{DS} is maximal.

Density and conductance of the open channel range can be determined as follows [12]:

$$d = d_0 - \sqrt{\frac{2 \cdot \varepsilon_0 \cdot \varepsilon_r}{q \cdot N_D} \left(U_{Bi} - U_{GS}\right)} \tag{2.3.1}$$

$$d_0 = \sqrt{\frac{2 \cdot \varepsilon_0 \cdot \varepsilon_r}{q \cdot N_D} \cdot U_P} \tag{2.3.1a}$$

$$U_P = U_{Bi} - U_T \tag{2.3.1b}$$

$$G_K = \frac{q \cdot n \cdot b \cdot d \cdot W}{L} \tag{2.3.2a}$$

$$G_K = \sigma \cdot \frac{d \cdot W}{L} \tag{2.3.2b}$$

d : open channel density
ε_0 : di-electric constants of the vacuum
ε_r : relative di-electric constants from GaAs (11 to 13)
U_P : total potential difference between completely opened and constricted channel /19
N_D : doping level in the channel

2.3.2 Structural element as Hall structure

According to Figure (2.3.1), the structural element is exposed to a homogenous transverse magnetic field. As a result the electric conductivity in the entire area between the drain and source is influenced. Evaluation of this conductivity variation as described in [4] is not limited to the channel, but rather includes the contact areas and the areas between the contacts. The influence of these dimensions diminishes according to how the

passage and contact resistances become negligible with regard to channel resistance. At voltages $U_{GS} \geq 0$ Volts the channel is wide open. Then, in spite of gate lowering, channel resistance is dimensionally equal to passage and contact resistance.

By superimposition of a small alternating voltage u_{gs} on the grid potential of the gate U_{GS} it is, however, possible, not for the entire open channel density d, but solely for the channel layer δ modulated by u_{gs} to be considered an effective Hall structure. It is necessary only to evaluate the additional alternating current i_{ds} flowing through u_{gs}.

/20

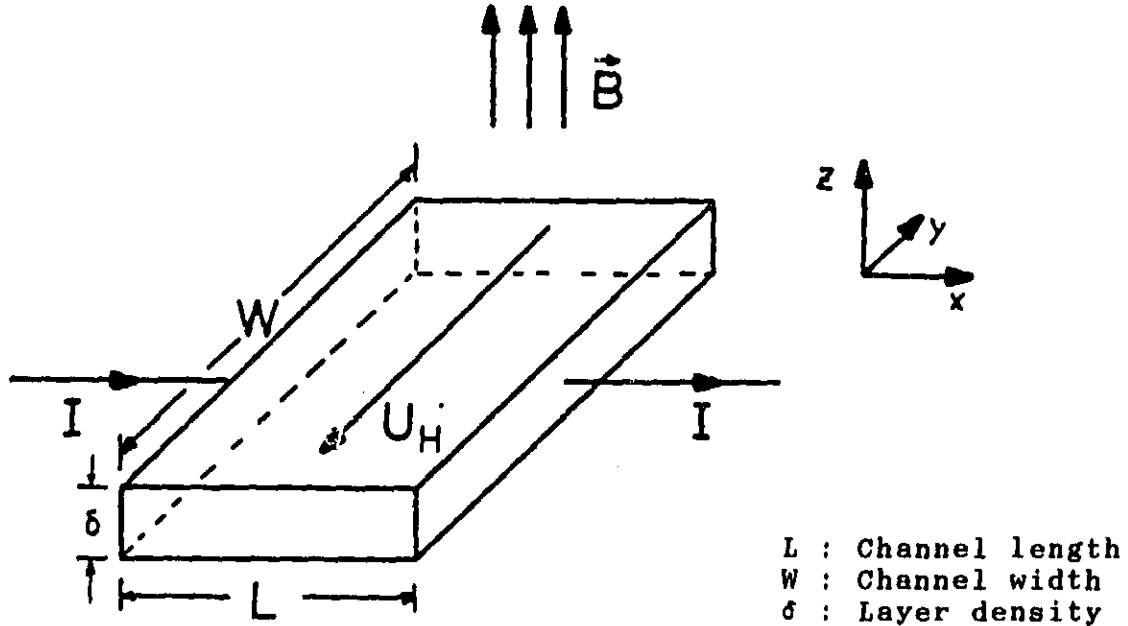

Figure. 2.3.2: Tolerance of effective Hall structure

In preliminary approximations it may be assumed that the length and width of the channel concur with those of the gate contact. For this reason the values ($L = 0.7\ \mu m$, $W = 300\mu m$) taken from Figure (2.3.1) can be used. The channel layer density is calculated with half of equation (2.3.1).

$$\delta = d(U_{GS} - u_{gs}) - d(U_{GS}) \qquad (2.3.4a)$$

$$\delta = \sqrt{\frac{2\varepsilon_0\varepsilon_r}{q \cdot N_D}} \cdot \left[\sqrt{U_{Bi} - U_{GS} - |u_{gs}|} - \sqrt{U_{Bi} - U_{GS}}\right] \qquad (2.3.4b)$$

Calculating on the basis of the MESFET data from Figure (2.3.1) and using the values:

$N_D = 0.5 \cdot 10^{18}\ cm^{-3}$
$u_{gs} = 50\ mV$

the density of the channel layer in the proximity of the gate $_{GS}$ = 0.5 V) is found to be:

$$\delta = 2\ nm$$

/21

In the proximity of SI (U_{GS} = -1.3 V) it is:

$$\delta = 0.6\ nm$$

For minimally doped MESFETs the density of the layer can increase to 6 nm. In comparison with the density of the right-of-way area (80 to 400 nm) these values are minute. Since resistance is reversely proportional to density, channel layer resistance is much greater than passage area and contact resistances.

On the basis of the geometry of Figure (2.3.2) a side relationship occurs, given as:

$$L/W = 0.0023$$

This value very nearly equates to the boundary case L/W = 0, which was used for the simplified evaluation of the geometric conductance reduction. The influence of the magnetic field on the conductivity of a thin channel layer in the structural element can, therefore, be described sufficiently well with the following expression (see Chapter 2.4):

$$\sigma(B) = \frac{\sigma(0)}{1 + b^2B^2} \tag{2.3.5}$$

2.3.3 Influence of magnetic fields on transconductance

/22

Up to this point it has been possible to determine the magnetic field dependency of the electric conductivity. The Magneto-transconductance-mobility-profiling procedure does not, however, depend upon conductivity measurements, but rather upon transconductance measurements. For this reason it is necessary to investigate how transconductance changes in magnetic fields.

According to equation (2.1.7) the definition of transconductance is realized by means of superimposition of the alternating voltage u_{gs} on the grid potential of the gate U_{GS}:

$$S = \lim_{\Delta U_{GS} \to 0} \frac{\Delta I_{DS}}{\Delta U_{GS}} \approx \frac{i_{ds}}{u_{gs}} \tag{2.3.6}$$

Chapter (2.3.2) already introduced the alternating voltage of the gate u_{gs}. It is necessary because it is used to evaluate a thin channel layer (locally resolved mobility profile) and the

influence of the right-of-way and contact resistances can be reduced. A transconductance measurement in accordance with equation (2.3.6) has the advantage that it produces a dimension which

--is only dependent upon i_{ds} and u_{gs}.
--guarantees that the evaluation limits itself to the thin channel layer.
--is plain and sensible.

The magnetic field dependency of the transconductance is determined by i_{ds}. The working point and the alternating current of the gate are independent of the magnetic field.

$$i_{ds}(t) = G_K(\delta, t)\ U_{DS} \tag{2.3.7}$$

In equation (2.3.7) it was taken into consideration that /23

--the work point lies in the starting range of the MESFET, so that the ohmic law is valid.
--the time independence of the current i_{ds} can be related back to the channel layer which has been modulated in the cycle of u_{gs}.

If one takes into consideration that the channel conductance is dependent upon the electrical conductivity in accordance with the following:

$$G_K(\delta) = \sigma \cdot \frac{\delta(t) \cdot W}{L} \tag{2.3.8}$$

then the following holds true for the relationship of the transconductance without magnetic field S(0) to the transconductance with magnetic field S(0):

$$\frac{S(0)}{S(B)} = \frac{i_{ds}(0)}{i_{ds}(B)} = \frac{\sigma(0)}{\sigma(B)} \tag{2.3.9}$$

The magnetic field dependency of the transconductance concurs with the dependency of the electric conductivity determined in Chapter (2.2). Integration of equation (2.2.15) leads to the measurement equation:

$$b = \frac{1}{B} \cdot \sqrt{\frac{S(0)}{S(B)} - 1} \tag{2.3.10}$$

2.4 Influence of idealization /24

Chapter (2.3) showed that the geometry of a GaAs-short channel-MESFET is suited for the utilization of the effect of the geometric conductance reduction. The effect of the conductance reduction could be carried over to the transconductance measurements. Cognizant of the geometry and physics of the real structural element, we shall now make a qualitative and, if

possible, quantitative analysis of errors which occur when adapting a MESFET to the idealizations of equation (2.2.15) and/or (2.3.10).

2.4.1 Finite geometry

Figure (2.3.2) presents a portion of the structural element which is responsible for the magnetic field dependency of the current i_{ds}. We have established the side ratio:

$$L/W = 0.0023 \qquad (2.4.1)$$

The equations

$$G_R(L/W,\ b\ ,\ B) = 1 + b_2 B_2 \qquad (2.4.2)$$

$$\sigma(0) = \frac{\sigma(0)}{1 + b^2 B^2} \qquad (2.4.3)$$

are valid under the given: /25

$$L/W \rightarrow 0 \qquad (2.4.4)$$

Equation (2.4.1) presents an error, whose influence on equation (2.4.3) must be investigated. The universal solution of the geometric function is:

$$G_R(L/W, \Theta_H) = \frac{W}{L} \cdot \frac{1}{\cos \Theta_H} \cdot \frac{Z_R}{N} \qquad (2.4.5)$$

Z_R and N are non-analytic soluble integral expressions. For this reason integration of equation (2.4.1) into equation (2.4.5) does not lead to an analytical calculation of the mistake through the finite side ratio L/W.

The following graphic solution of the geometric function serves for a qualitative analysis.

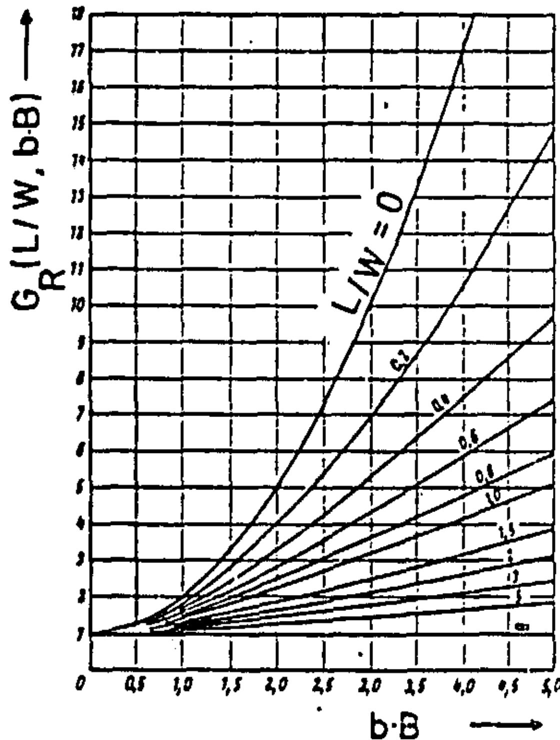

Fig. 2.4.1: Geometric function for resistance increase of right-angled semiconductor plates [2]

The representation of the geometric function shows very clearly how near the graph for L/W = 0.0023 lies on the graph of L/W = 0. It should, however, be pointed out, that the product b · B does not exceed the value 0.5. This value range is only insufficiently represented in Figure (2.4.1). The integral expressions in equation (2.2.5) are constant, so that the statement encountered in the aforementioned figure for a relatively high b · B, can be carried over to a lower value of this product. For this reason a noticeable error caused by the real side ratio L/W on equation (2.4.3) can be avoided. /26

2.4.2 Passage and contact resistance

For short-channel MESFETs in starting range the ohmic law is valid between the applied voltage U_{DS} and its resulting current I_{DS}. The drain-source current may be characterized by the following representation of a resistance replacement switch.

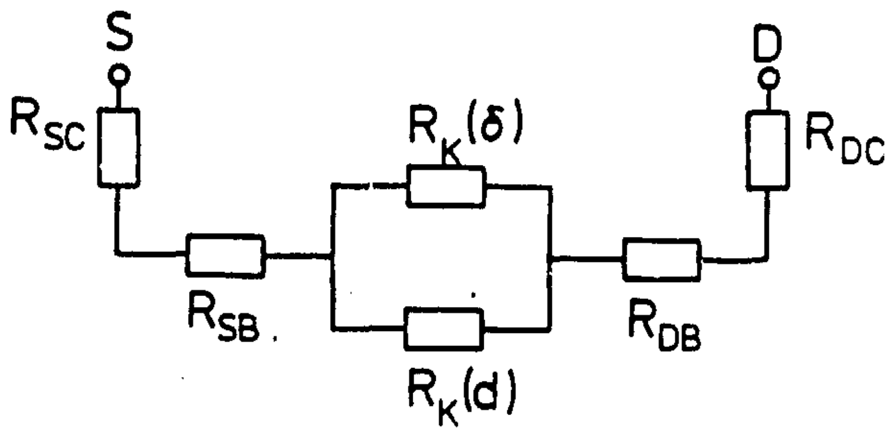

Fig. 2.4.2: Replacement switch representation characterizing the drain-source current

$R_K(\delta)$	:	Channel layer resistance modulated by u_{gs} /27
$R_K(d)$	:	Open channel resistance determined by U_{GS}
$R_{..C}$	:	Contact resistance of the drain/source contact
$R_{..B}$	:	Passage resistance between drain contact and channel or source contact and channel

The channel conductance in Figure (2.4.2) is represented by the parallel connection of $R_K(\delta)$ with $R_K(d)$. The superimposition of the gate's grid potential U_{GS} and its alternating voltage u_{gs} must be considered here. Since only the current portion i_{ds} is drawn upon for measuring transconductance, channel resistance $R_K(d)$ remains without influence. The following simplified representation of a replacement switch characterizing the alternating current i_{ds} results if the contact and passage resistances of the drain and source are combined into one contact and passage resistance.

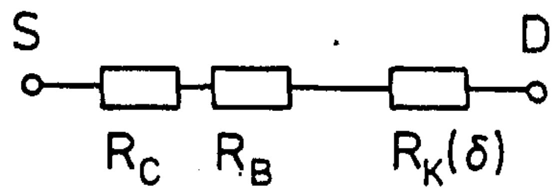

Fig. 2.4.3. Simplified representation of a replacement switch characterizing i_{ds}

On the basis of Figure (2.4.3) the influence of errors caused by passage and contact resistance can be investigated. The following relationship serves as a solution statement:

$$\frac{S(B)}{S(0)} = \frac{R(0)}{R(B)}$$

$$\frac{S(B)}{S(0)} = \frac{R_C + R_B + R_K(\delta)}{R_C(1+\sigma_C^2 B^2) + R_B(1+\sigma^2 B^2) + R_K(\delta)(1+\sigma_K^2 B^2)} \qquad (2.4.6)$$

b_K : Charge carrier mobility in the channel /28
b_B : Charge carrier mobility in the passage area
b_C : Charge carrier mobility in the contact area

This statement begins with the assumption that every resistance is subject to a geometric conductance reduction in the boundary case L/W = 0. A side ratio of 0.01 is not exceeded for the passage areas, so that the approximation is sufficiently fullfilled in all cases. Taking the contact area as a Hall structure is more problematic. Here, current flow and magnetic field are not always perpendicular to each other. It is also unusual to apply Hall structures to ohmic contacts. Nevertheless, the electric conductivity, which is described as analogous to semiconductor materials by means of mobility and concentration of the charge carriers, is completely dependent upon the magnetic field. The resulting side ratio concurs approximately with that of the passage areas.

For consideration of errors, therefore, a statement based on equation (2.4.6) is legitimate and can describe the influence of parasitic resistances on the equation

$$\frac{S(B)}{S(0)} \qquad \frac{1}{1 + b^2B^2} \tag{2.4.7}$$

An evaluation of equation (2.4.7) delivers an uncorrected value b for mobility in the channel, while an evaluation of equation (2.4.6) delivers a corrected value, the actual mobility in the channel. The error which is being sought results from an evaluation of equation (2.4.7). To this end the two equations are equated to each other:

$$\frac{1}{1+b^2B^2} = \frac{R_C + R_B + R_K(\delta)}{R_C(1+b_C^2B^2) + R_B(1+b_B^2B^2) + R_K(\delta)(1+b_K^2B^2)} \tag{2.4.8}$$

Transformations of the equation result in: /29

$$\frac{b_K}{b} = \sqrt{1 + \frac{R_C}{R_K(\delta)}\left(1 - \frac{b_C^2}{b^2}\right) + \frac{R_B}{R_K(\delta)}\left(1 - \frac{b_B^2}{b^2}\right)} \tag{2.4.9}$$

A simplification for small k can be carried out by means of Taylor series development. It is based on:

$$\sqrt{1+k} \approx 1 + 0{,}5 \cdot k$$

This approximation can be applied to equation (2.4.9), since the geometry guarantees, that

$$R_K(\delta) \gg R_B \approx R_C$$

$$\frac{b_K}{b} = 1 + \frac{1}{2}\frac{R_C}{R_K(\delta)}\left(1 - \frac{b_C^2}{b^2}\right) + \frac{1}{2}\frac{R_B}{R_K(\delta)}\cdot\left(1 - \frac{b_B^2}{b^2}\right) \tag{2.4.10}$$

The error is defined at:

$$f_b = \frac{b_K}{b} - 1 \tag{2.4.11}$$

A comparison with equation (2.4.10) gives us:

$$f_b = \frac{1}{2}\,\frac{R_C}{R_K(\delta)}\left(1-\frac{b_C^2}{b^2}\right) + \frac{1}{2}\,\frac{R_B}{R_K(\delta)}\left(1-\frac{b_B^2}{b^2}\right) \tag{2.4.12}$$

Discussion of equation (2.4.12):

Equation (2.4.12) consists of two correction terms. The left describes the influence of the contact areas, the right those of the passage areas. The direction of the influences is given by the relationship of the mobilities. The resistance relationship only has influence on the strength.

Ohmic contacts generally have a high concentration and a low mobility of charge carriers. b_C is therefore generally smaller than b, so that the first term is negative.

In passage areas the mobility is higher because of the /30 larger distance from the surface, so that the second term will be positive. The errors do not generally add up.

The resistance $R_K(\delta)$ is a function of the depth in the channel. At the gate contact δ is large and therefore resistance is small. As distance from the gate increases, δ decreases and resistance increases. For this reason the influence of mistakes caused by resistance relationships is greatest at the gate contact.

In the following we shall assume a quantitative mistake estimation. If we limit ourselves here to the passage areas, then this will be an estimation upwards, since the errors from the contact areas must be substra ted quantitively from it.

$$f_b < f_o = \frac{1}{2}\cdot\frac{R_B}{R_K(\delta)}\cdot\left(1-\frac{b_B^2}{b_C^2}\right) \tag{2.4.13}$$

At the gate contact b < b_B. Depending upon the profile, a drop in voltage up to half of the maximum value can result. The mobility b_B is an average dimension above the height of the passage areas and is not dependent upon the working point. From the primary approximation the following can be set:

$$b_{max} = b_B$$

The maximum mobility in the channel corresponds to the mobility of the passage areas. With the aforementioned assumptions, then, it is valid that:

$b_{min} = 0.5\ b_B$

The resistances are calculated according to equation (2.3.2):

$$R_K(\delta) = \frac{1}{n \cdot b \cdot q} \cdot \frac{L}{W \cdot \delta} \qquad (2.4.14a)$$

$$R_B = \frac{1}{n \cdot b_B \cdot q} \cdot \frac{2 \cdot l_B}{W \cdot h} \qquad (2.4.14b)$$

l_B : Length of the passage areas between contact and channel /31

h : Height of the passage areas

The factor 2 in the equation of the passage resistance considers the addition of the passage resistance between the gate and source and the gate and drain. Integration of the values L = 0.7 μm and a layer depth δ = 2.6 nm results in a resistance relationship:

$$\frac{R_B}{R_K(\delta)} = 2 \cdot \frac{b \cdot \delta \cdot l_B}{2 \cdot b \cdot h \cdot L} = 0{,}0046 \qquad (2.4.15)$$

Integration in equation (2.4.13) gives us an upward estimation of the mistake at the gate contact at

$$f_o = -14\%$$

This error decreases through the influence of the contact area. As distance from the gate increases, the number of errors decreases rapidly, since

-- layer density δ decreases.
-- b increases.

In the proximity of the semi-insulation material b decreases more drastically again, so that errors, in spite of higher resistance, increase again.

Exact error estimation is only possible on the basis of corresponding structural element data and their distribution in the channel. The principle influence will be examined in the following.

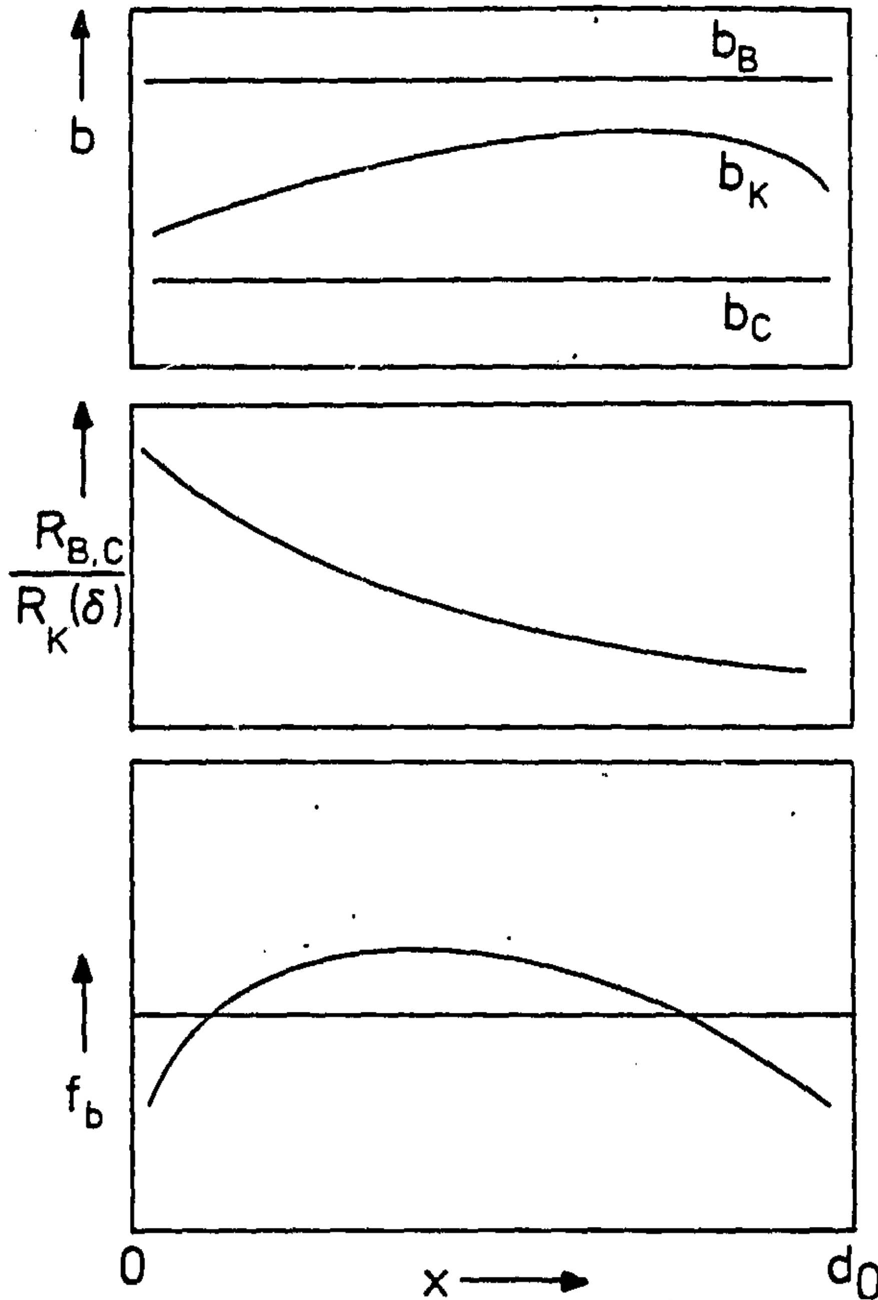

Fig. 2.4.4: Distribution of the error function f_b and its causes in the channel

An error boundary is cited in literature source [1]. This value is maintained in wide portions of the profile. A value of 10% may not be exceeded in the boundary layers.

2.4.3 Idealization of the geometry and summary observation of physical and geometric error influences /33

In Chapter (2.3.1) the area under the gate was defined as an active Hall structure. The geometric conductance reduction for this structure was then calculated according to

$$S(B) = \frac{S(0)}{1 + b^2 B^2}$$

With the exception of the approximation L/W→0, the Hall structure must have metallic contacts in order to fulfill the aforementioned equation ideally. A short circuit of the Hall structure and/or a forced right angle position of the electric field strength on the electrodes can only occur by means of very high contact conductivity. Establishment of such an ideal contact is not given in the MESFET. Nevertheless the connection of the thick passage areas ($h \approx 200$ nm) onto the thin channel layer ($\delta \approx 2.6$ nm) can be considered a relatively ideal contact. In the passage areas the electric current density is very much smaller and therefore

$$E_{yB} = R_H \cdot g_{xB} \cdot \sigma .$$

The y-components of the electric field strength are very small. Further, the geometric resistance effect weakens E_y in the passage areas with

$$1/W = 0.008$$

The connection from the passage area to the channel can be looked at as a boundary layer free of space charge, so that it is true that:

$$\operatorname{div} \vec{E} = 0 \qquad (2.4.16)$$

The tangential components of E are constant. Since the y-components of E are near zero in the passage area, the y-components in the boundary layer are minute as well. /34

An even more thorough consideration of these and other physical sources of errors would be beyond the scope of the present study. On the basis of the observations we have made thus far it is to be expected that according to

$$b = \frac{1}{B} \cdot \sqrt{\frac{S(0)}{S(B)} - 1} \qquad (2.4.17)$$

electron mobility can be measured with a high amount of precision. Nevertheless this relationship can only be valid with a high amount of surety if the experiment confirms its resultant equation:

$$S(B) = \frac{S(0)}{1 + b^2 B^2} \qquad (2.4.18)$$

The result of such an experiment is shown in the following figure.

/35

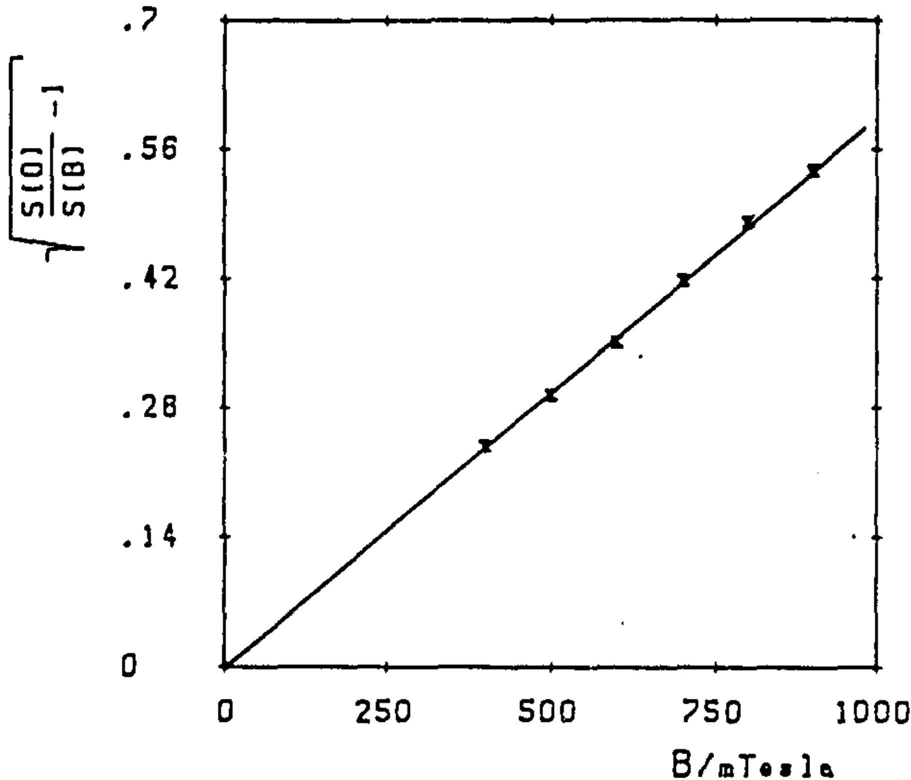

Fig. 2.4.5: Experimental confirmation of the evaluation equation

Over the magnetic flow density B we add $\sqrt{\frac{S(0)}{S(B)} - 1}$. A comparison with equation (2.4.17) results in a line equation with the gradient b.

$$\sqrt{\frac{S(0)}{S(B)} - 1} = b \cdot B \qquad (2.4.19)$$

If the graph in Figure (2.4.5) is an even one, then it is a proof for

-- the quadratic relationship between S(0) and S(B).
-- the independence of the mobility b from B in the exhausted range of the magnetic field.

Experimental control of the resultant equation is needed because of the varied causes of errors. An exact calculable /36 control of the error function f_b according to equation (2.4.12)

is not useful because of the high technical effort required to attain the structural element data which depend on the test and each respective working point. On the basis of the foregoing considerations the error boundary caused by physical idealization can be established at +/-5%.

3. Measuring room

/37

3.1 Measuring principle

In the following chapter we shall first summarize the resultant equations for the measuring procedure and then discuss the set up and the functioning of the measuring room.

To determine mobility in the channel we have the resultant equation

$$b = \frac{1}{B} \cdot \sqrt{\frac{S(0)}{S(B)} - 1} \qquad (3.1.1)$$

The equation determines mobility at a depth determined by the grid potential of the gate U_{GS}. By superimposition of the alternating voltage u_{gs} on the grid potential U_{GS} the thickness of the space charge zone d_R is modulated to its mean value. There is an alternating current i_{ds} which originally is connected with the modulated channel layer in the boundary between the space charge zone and the open channel. The transconductance measurement

$$S = \frac{i_{ds}}{u_{gs}} \qquad (3.1.2)$$

is strongly related to the modulated channel layer. A second (or more) transconductance measurement results when the test is subject to an homogenous magnetic field of the flow density B. With the data

-- S(0)
-- S(B)
-- B

equation (3.1.1) yields the mobility:

$$b = b(x_0) \qquad (3.1.3)$$

With the agreements of Figure (2.3.1) it holds for the depth coordinates x_0 that: /38

$$x_0 = d_R(U_{GS}) \qquad (3.1.4)$$

By varying the work points

$$0 < x < d_0 \quad (3.1.5a)$$

$$U_{Bi} > U_{GS} > U_T \quad (3.1.5b)$$

one can in this manner measure mobility at every depth of the channel. For clarity the measuring process is shown in the following flow diagram.

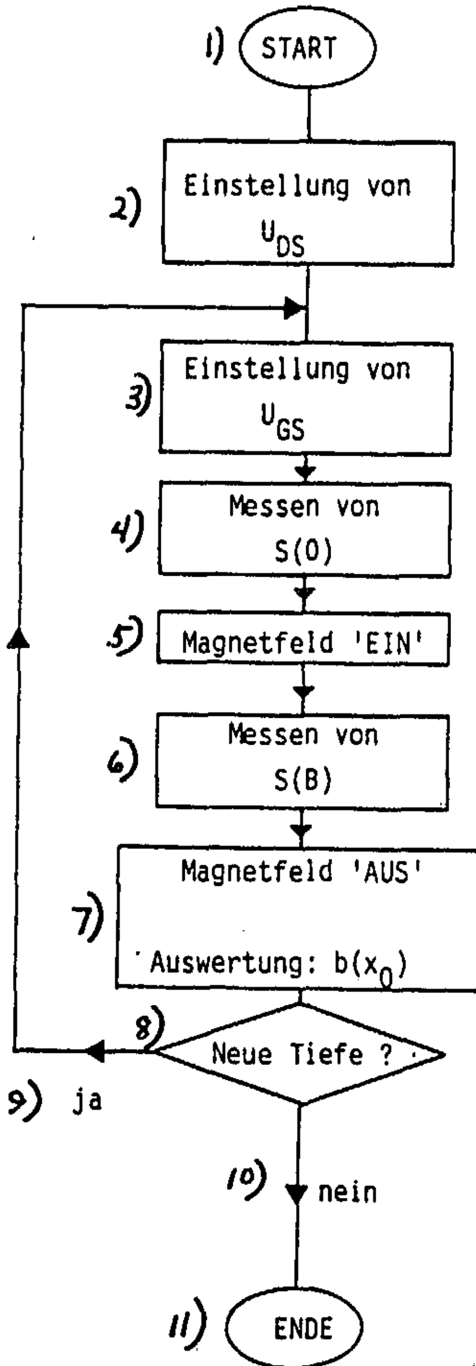

Key: 1) Start 2) Setting of U_{DS} 3) Setting of U_{GS} 4) Measurement of S(0) 5) Magnetic field "IN" 6) Measurement of S(B) 7) Magnetic field "OUT" Evaluation: $b(x_0)$ 8) New depth? 9) yes 10) no 11) End

Figure 3.1.1: Flow diagram of the measuring cycle

The following measuring device is required to carry out this measuring cycle: /40

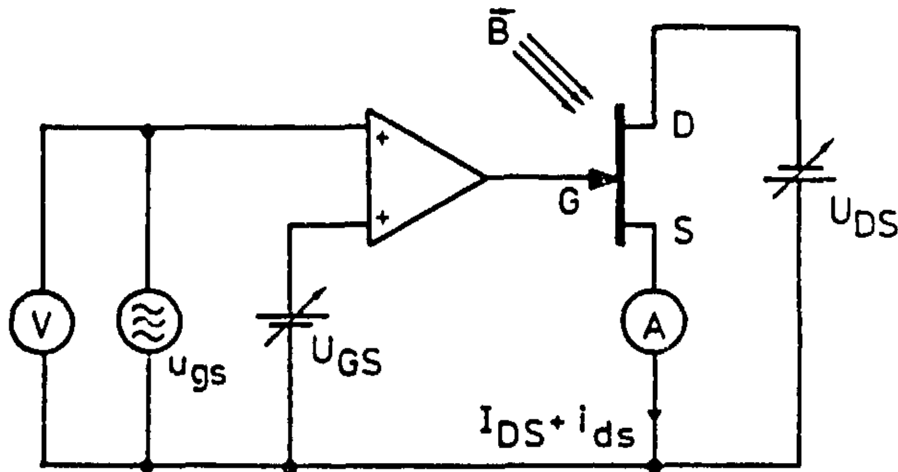

Figure 3.1.2: Model of a measuring device

The measuring device consists of:

- Adjustable direct voltage sources for the work points U^{GS}, U_{DS}
- Alternating voltage source u_{gs}
- Voltage meter for determining alternating voltage
- A device for neutralizing and determining channel current i_{ds}

To reduce errors the alternating current u_{gs} in accordance with equation (2.4.12) is set at approximately

$$u_{gs} = 50 \text{ mV} \quad (3.1.6)$$

In the starting range of a MESFET transconductance has a value of about:

$$S = 1 \text{ mS} \quad (3.1.7)$$

Using equation (3.1.2) these two values produce a current:

/41

$$i_{ds} = 50 \text{ } \mu\text{A} \quad (3.1.8)$$

Such a small current can no longer be measured accurately enough with a conventional ampermeter to permit its use in the measuring procedure. Further, a special filtering technique is required in order to separate the current i_{ds} from the equal portion I_{DS} and to reduse the noise effects. For this reason, a lock-in amplifier is installed in the measuring room.

The technical realization of the measuring device has the following configuration:

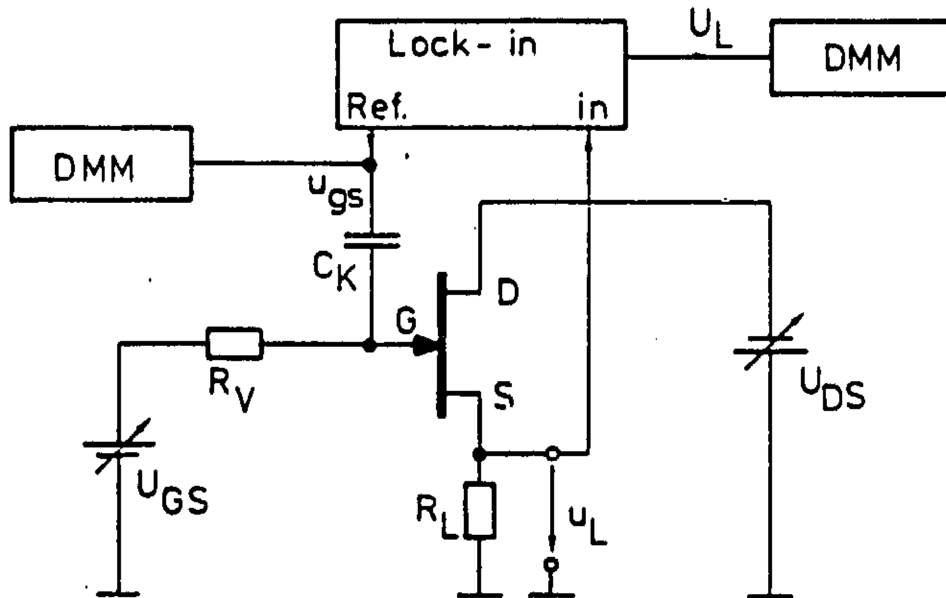

Figure 3.1.3: Technical realization of the measuring device

Application of a load resistance R_L becomes necessary, since the lock-in amplifier can measure only voltages. Over the load resistance R_L falls away voltage

$$U_L = i_{ds} \cdot R_L \tag{3.1.9}$$

The setting of R_L is so small that the current i_{ds} is not diminished. /42

3.2 Measuring equipment and voltage supply

3.2.1 Lock-in amplifier

The "Dynatrac 393" lock-in amplifier is the central measuring instrument of the measuring device. An evaluation of the physical measuring principle is possible only using this type of measuring technique. The following figure shows a detail of the application range of this measuring instrument.

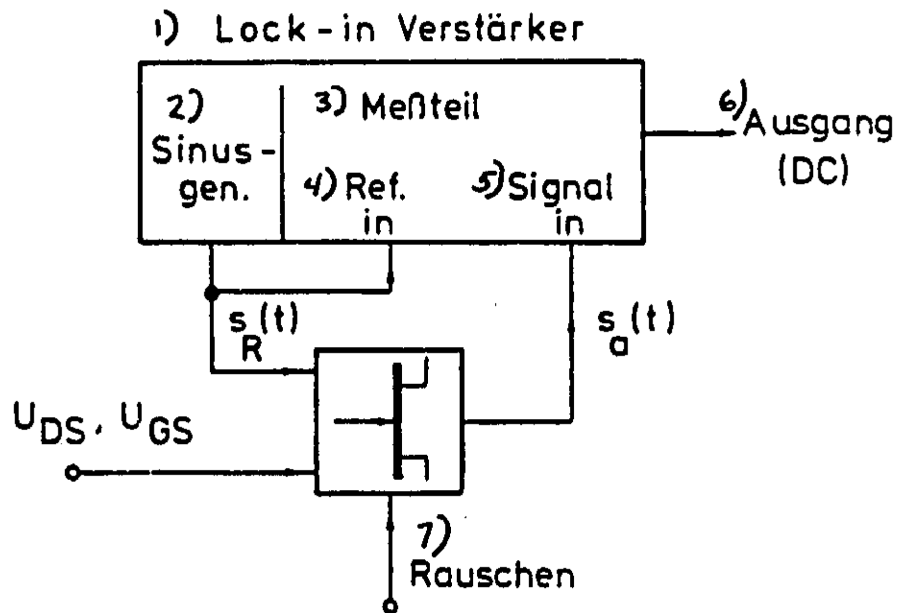

Figure 3.2.1: Application range of the lock-in amplifier
Key: 1) Lock-in amplifier 2) Sine generator 3) Measuring part 4) Reference in 5) Signal in 6) Exit 7) Noises

In the measuring instrument a comparison between the reference signal and the measuring signal takes place according to the following principle: /43

The phase regulating cycle in the lock-in shift phases the reference signal $S_R(t)$ until the product

$$s_R(t-\tau)\cdot s_a(t)$$

reaches a maximum. At the maximum state of the product both signals have the following per unit time course:

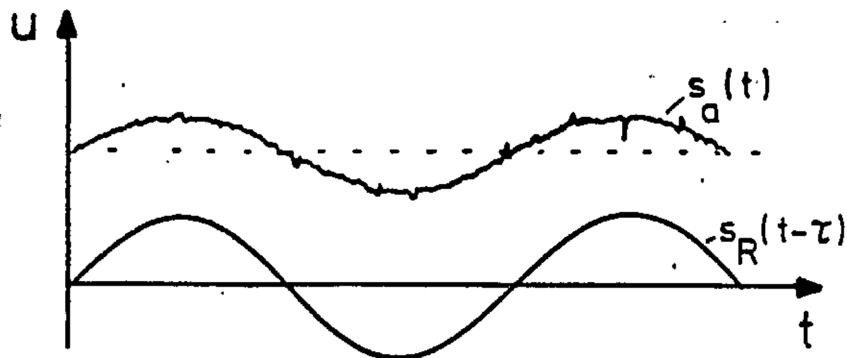

Figure 3.2.2: Comparison of reference and entrance voltage of the lock-in amplifier

Over a full period the product totals:

$$\frac{1}{T}\int_{t}^{t+T} s_R(\mu-\tau)\cdot s_a(\mu)\, d\mu$$

In the process, all portions fall out

--whose mean value over T is different from zero (equal portion).
--whose frequency is a multiple of the basic frequency (harmonic distortions).

Further, the signal/noise power ratio is optimum, since, analogous to the technique of the appropriate filter, signal portions with the highest correlation to the reference voltage demonstrate a maximum upward integral total. Ideally, white noise will be eliminated. /44

The output of the lock-in amplifier is a normalized direct voltage of the form:

$$U_L = F\left\{\frac{s_R(t-\tau)\cdot s_a(t)}{s_a(t)}\right\} \qquad (3.2.1)$$

The signal dimension $s_a(t)$ is composed of the equal portion I_{DS} R_L and the alternating portion i_{ds} R_L. In practical use there occur alternating currents of

3 to 300 μA

which must be measured with an accuracy of approximately 1%. Further, the channel resistance $R_K(d)$ lies in the range of approximately 30 to 100 ohms. The author is unaware of any conventional measuring instrument which is capable of this measuring task under the given circumstances.

The lock-in amplifier cannot measure direct currents, which is the reason that a load resistance R_L was applied in the drain-source cycle. Analogous to equation (2.4.12) R_L brings about an additional error at:

$$f_{R_L} = \frac{1}{2}\cdot\frac{R_L}{R_K(\delta)} \qquad (3.2.2)$$

R_L is kept at such a dimension (1 ohm), that the error does not generally go over 2%. The current i_{ds} can be produced from

$$i_{ds} = \frac{u_L}{R_L} \qquad (3.2.3)$$

with sufficient accuracy. U_L is the decrease in alternating voltage, which causes i_{ds} on the load resistance R_L.

The exit of the lock-in amplifier is a direct voltage proportional to U_L: /45

$$U_L = \frac{|u_L|}{S_E} \cdot 10\,V \qquad (3.2.4)$$

S_E is the entrance sensitivity set on the lock-in. It covers the value ranges:

$$0.1\ \mu V < S_E < 3\ V$$

The measurement accuracy is given by the producer at:

1%	Amplifier errors
0.05 %/K	Temperature drift

The filter selectivity amounts to 12 dB/octave.

3.2.2 Keithley digital multimeter

The measuring room contains two Keithley digital multimeters, the model "177 Microvolt DMM" and "179 TRMS DMM". Both models are compatible with IEC-Bus.

Model 177:

Assignment:	Measuring alternating voltage of gate u_{g0} and IEC-Bus cut-off position
Error:	0.9% (at 50 mV)
Entrance:	10^6 ohms/ 75 pF

Model 179 TRMS: /46

Assignment:	Measuring exit direct voltage of lock-in and IEC-Bus cut-off position
Error:	0.05% (at 10 Volt DC)
Entrance:	10^6 ohms/ 75 pF

3.2.3 Voltage supply

According to Figure (3.1.2), the direct voltages U_{GS} and U_{DS} are needed along with the alternating voltage of the gate u_{gs}. The alternating voltage generates a sine oscillator in the Dynatrac 393 lock-in amplifier.

Sine oscillator:

Frequency:	0.1 to 10 KHz (here 1 KHz)
Exit:	0 to 1 V at 1000 ohms
Error:	2% harmonic distortion, drift (see Chapter 4.1.4)

The IEC-Bus compatible two-channel voltage source "Rhode & Schwarz NGPS" serves as the direct voltage supply. The following data are valid for the "LOW" range.

Direct voltage source:

Voltage:	+/- 16.835 V
Current:	100 mA (130 mA current limit)
Error:	So small that the direct voltage supply can be considered ideal

3.2.4 Test circuit

/47

The technical measuring circuit calls for a load resistance R_L in the drain-source circuit and a switch for the feed-in of the gate voltage $U_{GS} + u_{gs}$. Since load resistance R_L (1 ohm) is very small, already small overvoltages lead to high currents and with them to destruction of the structural element. The cause of such voltages are:

- manual errors
- switching the voltage sources on and off

The following construction was developed for the protection of the test and as technical measuring wiring:

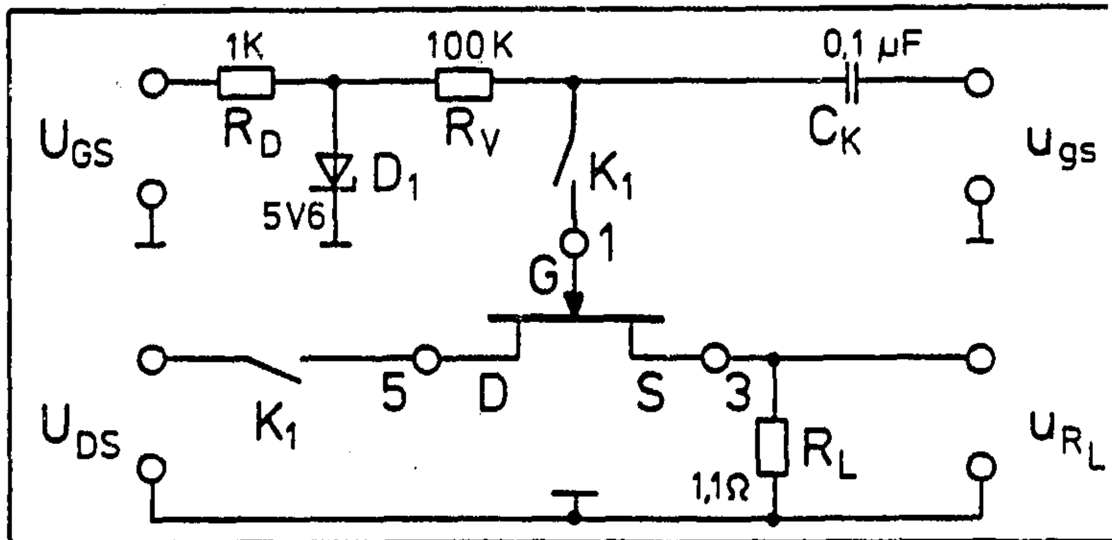

Figure 3.2.3: Test circuit

The R-C combination R_V C_K provides for feed of gate voltage U_{GS} + u_{gs}. R_V prevents a short circuiting of the alternating voltage u_{gs} over the direct voltage source U_{GS}. The condensor separates the direct voltage from the alternating voltage generator. An R-Zener breakdown is installed at the gate entrance U_{GS}. /48

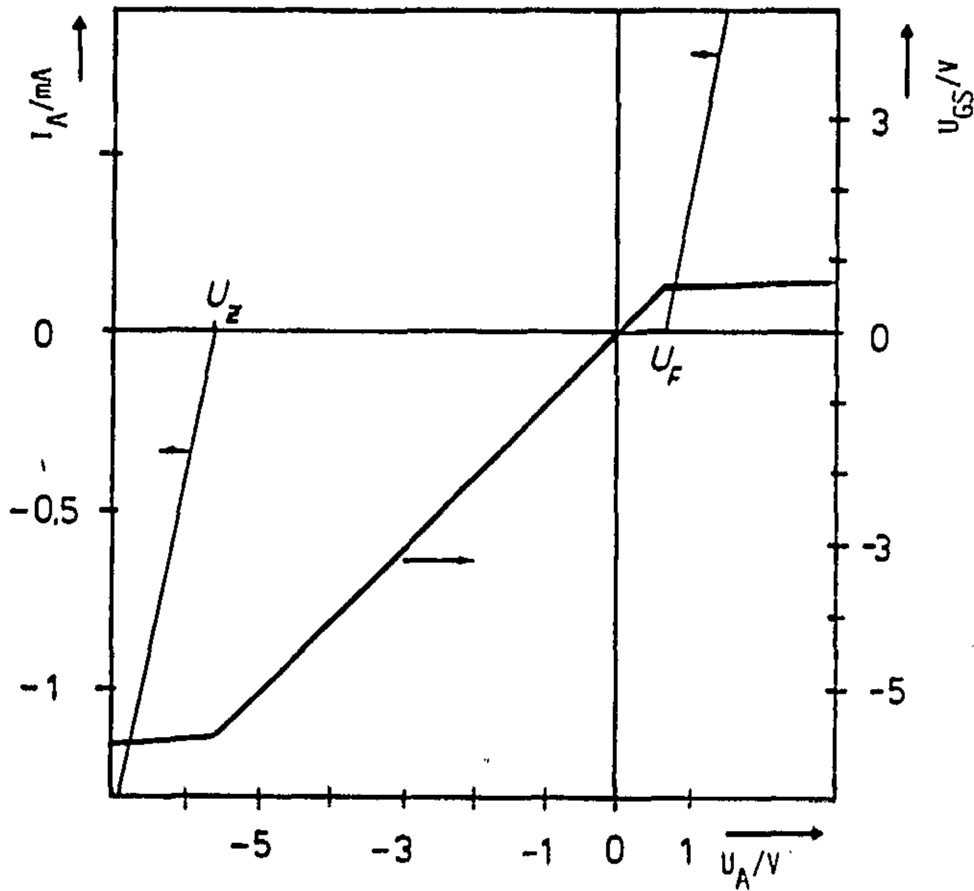

Figure 3.2.4: Acceptable value range of the gate-source voltage

The circuit causes the voltage U_A established from U_Z to U_F to be equal to the actual voltage at the gate. Voltages which lie above this value range are short circuited. The measuring range of U_{GS} looks like this:

$$+0.5 \text{ V} < U_{GS} < -5 \text{ V} \tag{3.2.5}$$

This condition is satisfied when U_F = 0.6 V and U_Z = 5.6 V.

A further protection precaution is the relay K_1. It is turned on directly by the measuring program and first establishes the /49 voltages at the drain and gate when the start-up process has been completed. After every measurement the relay once again separates the test from the voltage supply.

These precautions are necessary and effective to protect the test against voltage peaks, which occur during switching, particularly when turning off the direct voltage source, and can lead to destruction of the test.

The test circuit is the distributor position for the entire measuring construction. It is essentially responsible for the ease in inspecting the measuring room. This is made clear by the following figure:

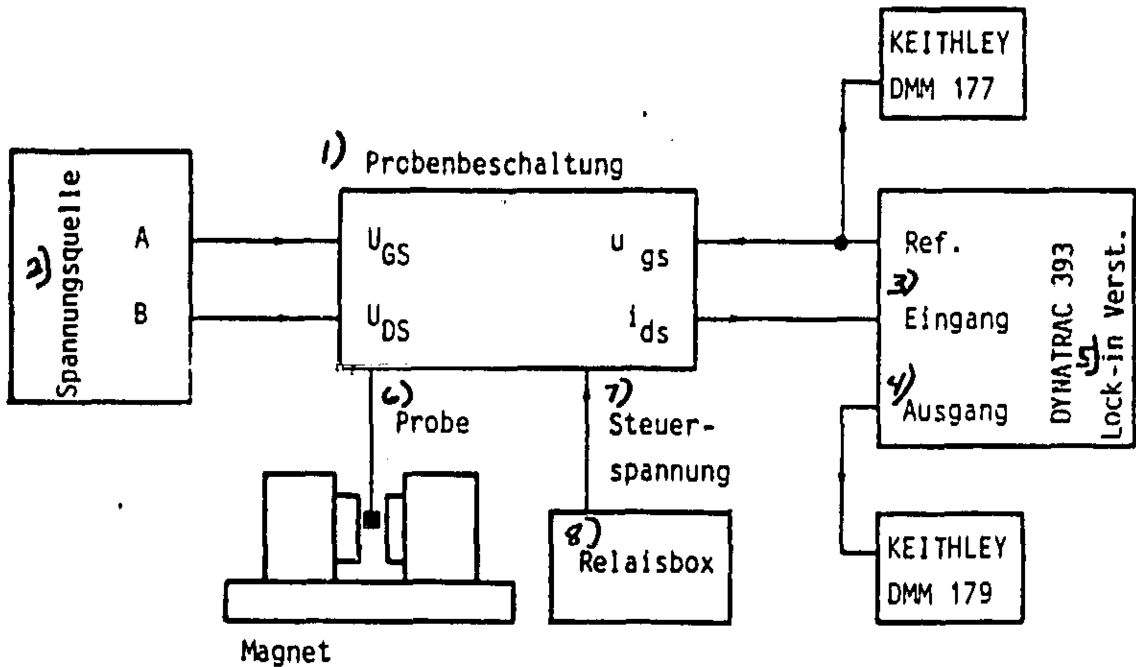

Figure 3.2.5: The test circuit in the block circuit of the measuring device
Key according to number: 1) Test wiring 2) Voltage source 3) Entrance 4) Exit 5) Lock-in amplifier 6) Test 7) Control voltage 8) Relay box

3.3 Magnetic field regulating circuit /50

Figure (3.1.3) shows the most detailed description of the technical realization of the measuring device to date. Nevertheless, the central calculation control (Chapter 3.4) and the adjustment of the magnetic field are lacking.

It is, however, precisely the adjustment of the magnetic field which is of particular importance in constructing the measuring room. The exact measurement of magnetic flow density is quite involved. Furthermore, there are certain requirements which must be maintained:

-- Adjustment of a variety of magnetic field sizes during a measuring cycle

-- The most exact adjustment possible

-- Fully automatic performance of the adjustment procedure by means of a terminal

In Chapter (2.4) we called for technical measuring control of the validity of the initial equation

$$S(B) = \frac{S(0)}{1 + b^2 B^2} \qquad (3.3.1)$$

This control should take place through verification of the linear connections

$$b \cdot B = \sqrt{\frac{S(0)}{S(B)} - 1} \qquad (3.3.2)$$

$$m \cdot x = y \qquad (3.3.3)$$

In order to obtain the settings of both magnetic field values ($B=0$, $B=B_0$), which suffice for evaluation of equation (3.3.1), many (in practice n=5 to 10) varied magnetic field values are set and used to measure the corresponding transconductances $S(B_k)$. /51

After the completion of a cycle, n-value groups of the form:

k; B_k; $S(B_k)$

are available. There data are evaluated by means of a linear regression (see Chapter 4.1.3.2) to a line equation according to equation (3.3.2).

This cycle must be repeated for every point on the mobility profile. For a complete profile the result is between 50 and 200 magnetic field adjustments, which by manual adjustment would require an operator to be present in the measuring room throughout the entire measuring time. Furthermore, such adjustment is very tiring. The error boundary acceptable for the adjustment value is subjective and different for every adjustment.

For this reason the following "digital" magnetic field regulation is set for the measuring device.

/52

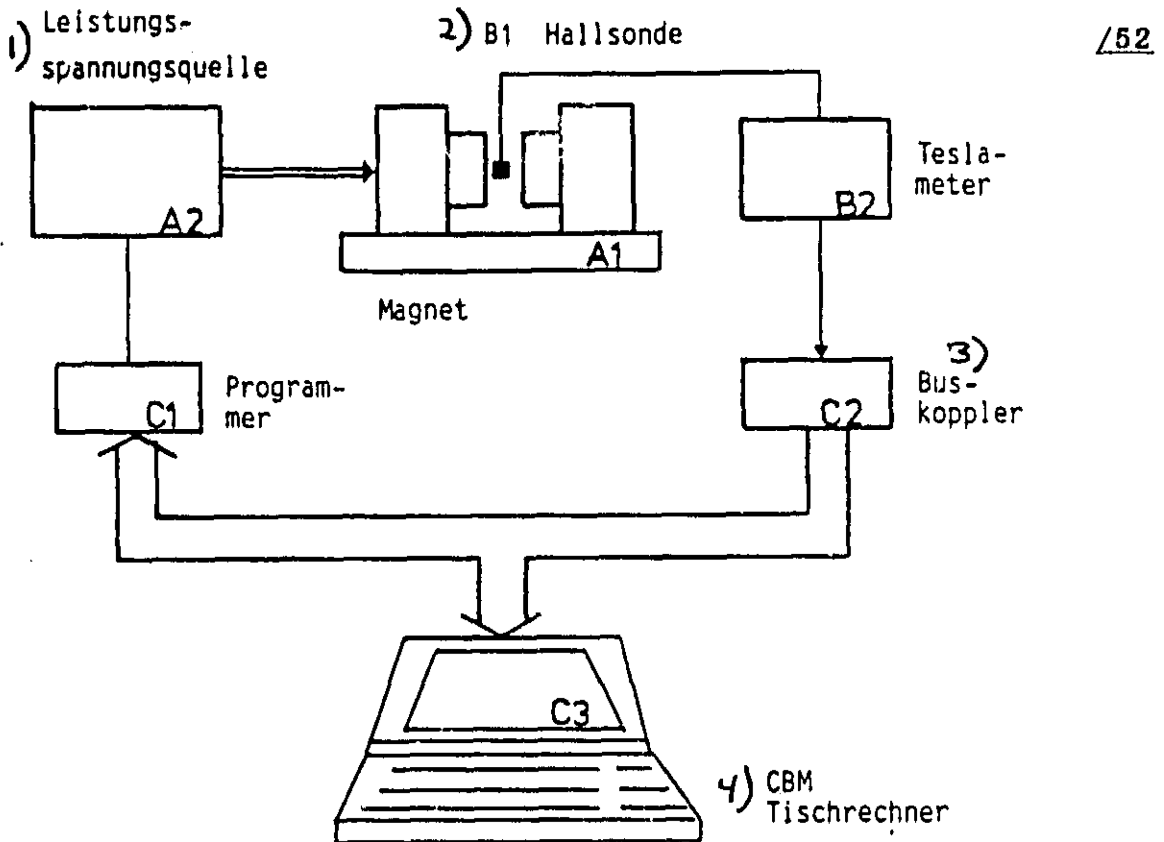

Figure 3.3.1: Block circuit for digital magnetic field regulation
Key: 1) Output voltage source 2) B1 Hall probe 3) Bus coupler 4) CBM terminal

3.3.1 Magnetic field regulating circuit instruments

The regulating circuit consists of three groups:

Group A: Generating elements
A1: Bruker magnet B-E 10B8
A2: Systron Donner Power Supply M7060-30

Group B: Measuring instruments /53
B1: Hall probe
B2: Tesla meter Systron Donner 3102 A

Group C: Adjustment parts and regulators
C1: Commander Systron Donner P1
C2: Instrument coupler ICS 4880
C3: Terminal CBM 4032

The elements of group A produce a relatively homogenous magnetic field up to a maximum of B_{max} = 1 tesla in an air gap of approximately 6 cm width. Group B facilitates measuring the actual value of B. It consists of a Hall probe, which transmits

a magnetic field proportional Hall probe to the second instrument of the group, the tesla meter. This instrument is calibrated on the Hall structure and converts the Hall voltage into a value of the magnetic flow depth. Magnetic field measurements are generally much more difficult and imprecise than electric measurements. Nonetheless, the combination used in this measuring room are considered quite good. The practical precision with which the line equation (3.3.2) can be satisfied has helped reduce the justifible prejudices against magnetic field measurements. For this reason, the error boundary of the producer can be incorporated:

$$f_T = 1\% \qquad (3.3.4)$$

Group C consists of converters C1, C2 and the logical element of a computer terminal. C1 converts a decimal number from 0 to 9999 into a control voltage U_{St} of 0 to 10V. U_{St} controls the voltage source A2 from 0 to 100% of its maximum voltage. The smallest magnetic field variation amounts to 0.01% corresponding to 0.1 mT. This ensures that the adjustment of every B-value is "ideally" possible. C2 allows the IEC-Bus terminal to read the digital tesla meter results. /54

3.3.2 Magnetic field regulation

The elements of Group A, B and C are connected to a regulating circuit.

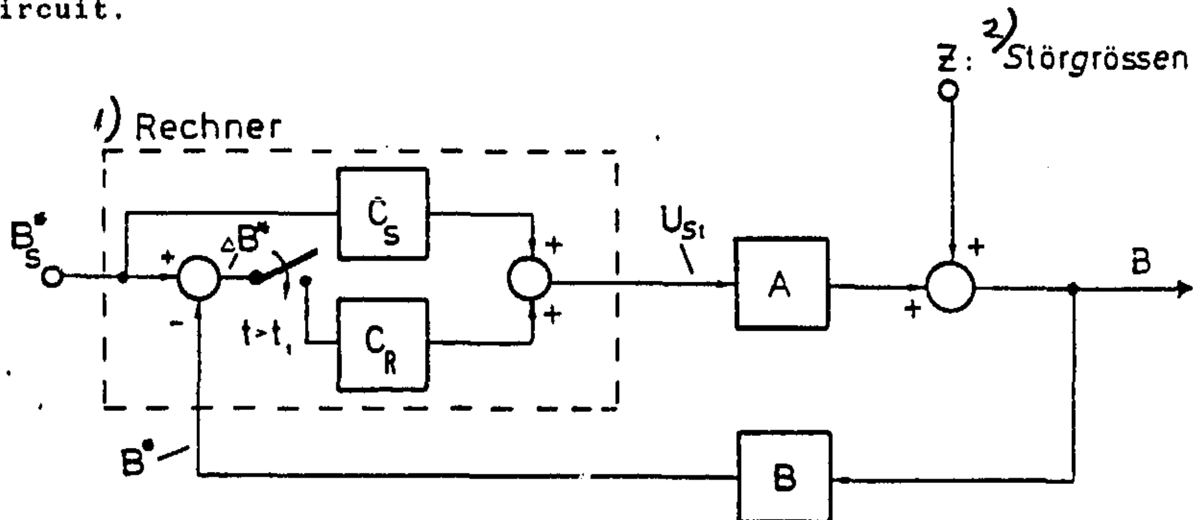

Figure 3.3.2: Magnetic field regulating circuit
Key: 1) Calculator 2) Disturbance dimensions

The figure shows a technical regulating representation as the schematic form of a single regulating circuit. The assignment and function of the terminal, the analogous/digital converter (A/D converter) and the D/A converter especially are strongly schematicized. Blocks A, B, C_S and C_R correspond to the

component groups listed in Chapter (3.3.1) with the conversion factors:

$$f_A, f_B, f_{C_S}, f_{C_R}$$

The dimensions with (*) are digital. Considering the great effort required for a technical regulating consideration of the "dead periods" using data recording and A/D and/or D/A conversion, dynamic regulation is abandoned. Since A/D and D/A conversion can be considered ideal, the problem of conversion will not be dealt with henceforth. /55

There are two steps in the construction of a regulator circuit in accordance with Figure (3.3.2)

1. Assumption of transfer factors f_A and f_B, which are given in the process and are immutable

2. Calculation and realization of the transfer factors f_{C_S} and f_{C_R} according to the points given in 1.

Regarding 1.):

The transfer function f_B describes the technical measuring composition and conversion of the actual value of B. Since no problems with the A/D conversion or technical measuring errors are observed here:

$$f_B = 1 \qquad (3.3.6)$$

Transfer function f_A describes the conversion of the dimension U_{St} into an actual value of B:

$$f_A: \quad U_{St} \rightarrow B$$

$$B = f_A(U_{St})$$

Function f_A was assumed by technical measurement in the measuring room: /56

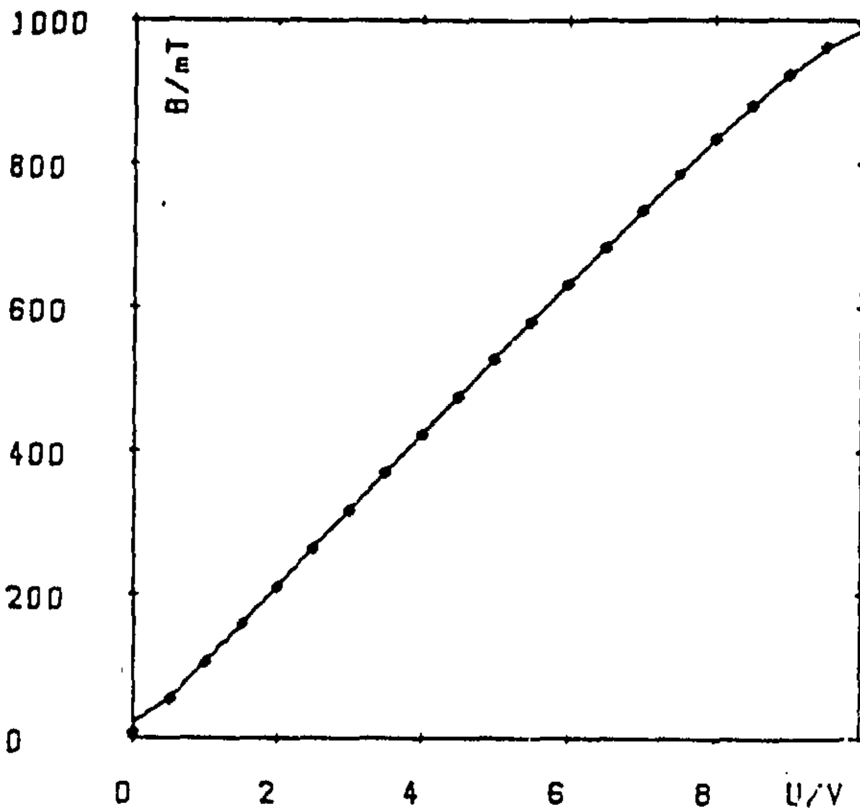

Control voltage

Figure 3.3.3: Transfer function of instrument group A

Regarding 2.):

The processes on the regulator circuit are differentiated according to times:

$t < t_1$: Control
$t > t_1$: Regulation

t_1: Conversion time of a real value of B in the first, error-ridden actual value of B

In accordance with Figure (3.2.2) the following relationship is valid for $t < t_1$:

/57

$$B = B_S \cdot f_{C_S} \cdot f_A + Z \qquad (3.3.7)$$

The term Z is an additional disturbance dimension, which must be stabilized. The pure control already works optimally, whenever the following is valid:

$$B = B_S + Z \qquad (3.3.8)$$

By means of comparison the dimensioning specification is attained:

$$f_{C_S} = (f_A)^{-1} \qquad (3.3.9)$$

Transfer function f_A as well as its inversion are not analytical functions. For this reason a solution of equation (3.3.9) was found by integrating pairs of value from Figure (3.3.3) into the statement:

$$f_{C_S}(B) = a_1 \cdot B + a_2 \cdot B^2 \qquad (3.3.10)$$

The results are:

$$a_1 = 8.606 \cdot 10^{-3} \text{ V } (mT)^{-1} \qquad (3.3.11a)$$

$$a_2 = 1.394 \cdot 10^{-6} \text{ V } (mT)^{-2} \qquad (3.3.11b)$$

At $t = t_1$ the real value of the magnetic flow depth was converted into an actual value:

$$B = B_S + Z \qquad (3.3.12)$$

The switch in Figure (3.2.2) is reversed; the regulator circuit is closed. The assignment of part C_R takes the dimension placed at the entrance:

$$\Delta B = B_S - B$$

and generates a correction dimension from it:

/58

$$f_{C_R}: \Delta B \longrightarrow \Delta U_{St}$$

The following condition must be satisfied:

$$f_A(U_{St} + \Delta U_{St}) = B + \Delta B$$

Function f_A is linearized at the working point:

$$f_A(U_{St} + \Delta U_{St}) \approx f_A(U_{St}) + \Delta U_{St} \cdot \frac{\partial f_A}{\partial U_{St}} \qquad (3.3.13)$$

Now the observations from equation (3.3.7) to (3.3.11) are applied to the changes B, U_{St}:

$$f_{C_R} = \Delta B \cdot \frac{\partial f_A^{-1}}{\partial B} \qquad (3.3.14)$$

Integration into equation (3.3.10) results in

$$f_{C_R} = \Delta B \cdot (a_1 + 2\, a_2 \cdot B) \qquad (3.3.15)$$

with a_1 and a_2 in accordance with equation (3.3.11).

With that the regulator circuit is completely dimensioned. Control and regulator functions f_C are realized by placing the functions into the measuring program of the computer in accordance with equations (3.3.15) and (3.3.10).

Regulation is considered complete when regulator error

$$\Delta B = B_S - B$$

falls below a certain level (1 to 3%). The following figure shows the per unit duration of the dimensions affected by regulation:

/59

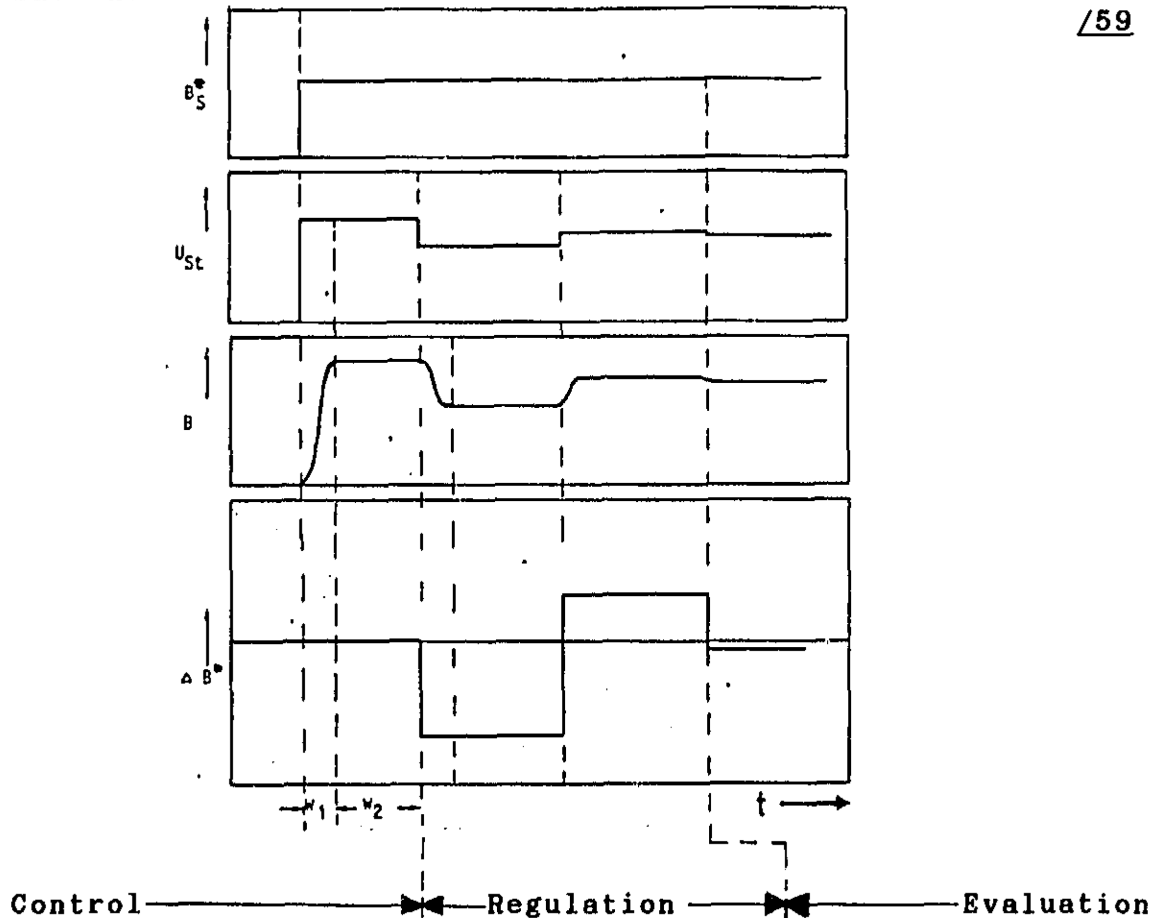

Figure 3.3.4: Time plan of the magnetic field regulation

W_1: Waiting time for adjustment of the magnetic field value
W_2: Assumption of the measured value of B

The other waiting times (A/D conversion) can be omitted because of W_1 and W_2.

3.4 Measuring room automation /60

In the previous chapter a portion of measuring room automation, the magnetic field regulation, was described in detail. As we saw there, the following points indicate the need for automation.

-- The amount of operator time is considerably reduced, since plotting of a highly solvable mobility profile can take many hours.

-- Work in the measuring room is very monotonous. This leads to a reduction in attention and to error conditions.

-- Data recording, data assurance, and evaluation are assumed by a computer.

-- The ability to reproduce measurement results is considerably increased.

The two last points increase measuring room measurement precision and dependability. The computer can calculate even monotonous mathematical algorithms, leading to a reduction in errors which is absolutely necessary for the measuring procedure (Chapter 4.1.3).

The measuring program can be structured as follows: /61

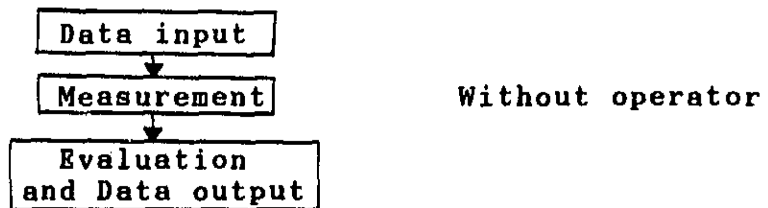

Figure 3.4.1: Structure of computer controlled measuring program

Upon data input, all variable parameters on the special test are determined. After completion of this phase, the terminal should have received all necessary information and the measuring room should be fully prepared to allow the second phase to proceed without an operator. An interruption of the measuring program should occur only when

-- Boundary data is surpassed
-- Errors occur in the measuring construction
-- The adjustment of measuring instruments must be corrected manually

The last point refers to the limitations of automation. In the case of the measuring device, this situation occurs upon correction of the entrance sensitivity of the lock-in amplifier. If transconductance in the channel radically decreases to SI, then the entrance sensitivity of the measuring instrument must be reset. Complete automation is possible only if all instruments utilized in the measuring room can be controlled centrally from the terminal. A programmable lock-in amplifier does not exist at the present time.

Development of automation in the measuring room for magneto-transconductance-mobility-profiling has progressed in proportion to the availability of measuring instruments which may be adapted to the IEC-Bus. In developing programs, particular emphasis has been placed on avoiding a complete interruption of measurement, with the terminal containing directions for resumption of the measuring procedure. /62

Example: Initial voltage of the lock-in U_L falls below 20% of total oscillation!
The technical measuring error threatens to become too large.

1. The computer stops the measurement just before taking in a new mobility number in order to avoid errors caused by measuring range shifts during an evaluation.

2. Computer instruction: "Correction of lock-in entrance sensitivity!"

3. The operator corrects the measuring range.

4. Computer asks: "Sensitivity μV?"
Operator inputs corrected value.

5. Measuring program continues!

This small example may clarify the procedure of logical measuring room supervision. We now turn to the complete data technical cabling of the measuring room.

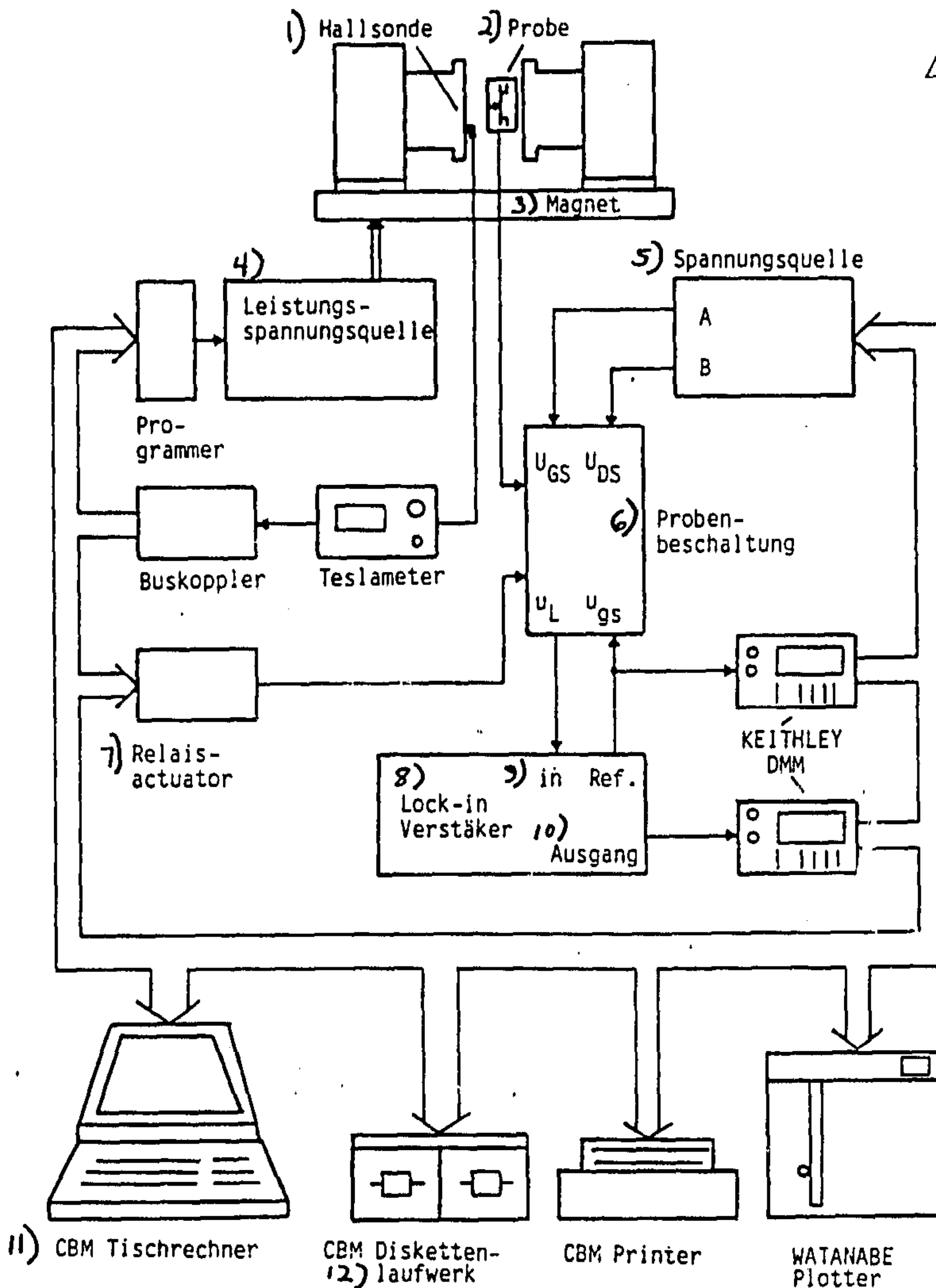

Figure 3.4.2: Entire block circuit of measuring room (Key on following page)

Key to Figure 3.4.2: 1) Hall probe 2) Test 3) Magnet 4) Output voltage source 5) Voltage source 6) Test circuit 7) Relay actuator 8) Lock-in amplifier 9) In Reference 10) Exit 11) CBM terminal 12) CBM CBM diskette drive assembly

4 Measuring technique

/64

4.1 Error observation

In our introduction to the measuring room in Chapter (3) it already became evident from the choice of modern and highly precise measuring instruments that the measuring procedure is highly sensitive to errors. Here we deal primarily with the imprecisions of measuring instruments and their influence on errors in the results investigated. An essential difficulty in constructing the measuring room consists of minimizing errors caused by the measuring instruments. This task has been solved on an engineering level, that is, the dominant error influences here have been reduced to a level equal to those of other errors.

4.1.1 Sources of errors

Basically all of the instruments involved in the measuring room may cause errors. In order to attain more meaningful observation of errors, we direct our attention to the essential parameters and their errors. These parameters are contained in the initial equations:

$$S(B) = \frac{S(0)}{1 + b^2 B^2} \qquad (4.1.1a)$$

/65

$$S = \frac{\mu_L}{R_L \cdot \mu_{gs}} = \frac{U_L \cdot S_E}{R_L \cdot \mu_{gs} \cdot 10V} \qquad (4.1.1b)$$

Both of these equations result in the evaluation equation of the measuring procedure which occurs independently of the error-laden dimensions occurring in the measuring room:

$$b = \frac{1}{B} \cdot \sqrt{\frac{U_L(0)}{U_L(B)} - 1} \qquad (4.1.2)$$

The goal of error observation is to minimize the error boundary of b, and, if possible, to record it in numerical values. Working from equation (4.1.2) we shall limit ourselves in the following to error observation in:

-- U_L: Lock-in initial voltage
-- B: Magnetic flow depth

Sources of error for these parameters are:

-- Lock-in amplifier
-- Hall probe/Tesla meter

The error influence of the voltage sources for U_{GS} and U_{DS} can be ignored. The same is true for all digital operations of the computer and the converters. Because of reference voltage drift these will be considered by themselves in Chapter (4.1.4).

4.1.2 Error sensitivity /66

Up to the first term, a Taylor succession serves as a starting point for the influence of parameter errors on end results:

$$b = b_0 + B \cdot \frac{\partial b}{\partial B} + U_L(0) \cdot \frac{\partial b}{\partial U_L(0)} + U_L(B) \frac{\partial b}{\partial U_L(B)} \qquad (4.1.3)$$

The partial derivatives can be obtained with equation (4.1.2). Here, for relative error:

$$\frac{b - b_0}{b_0} = -1 \cdot \frac{\Delta B}{B} + \frac{1}{2} \frac{U_L(0)}{U_L(0) - U_L(B)} \cdot \frac{\Delta U_L(0)}{U_L(0)} - \frac{1}{2} \underbrace{\frac{U_L(0)}{U_L(0) - U_L(B)}}_{E_i} \cdot \underbrace{\frac{\Delta U_L(B)}{U_L(B)}}_{f_i} \qquad (4.1.4)$$

This equation has the form:

$$f_b = \sum_{i=1}^{3} E_i \cdot f_i \qquad (4.1.5)$$

E_i : Sensitivity factor
f_i : Relative parameter error

Relative parameter error f_i corresponds to measuring instrument tolerance, while E_i gives the influence of parameter error on the error in the end result. Since all of the sum terms can have different signs (ideally being normally distributed), the amount of the error can be assumed.

$$f_b = \sqrt{\sum_{i=1}^{3}(E_i \cdot f_i)^2} \qquad (4.1.6)$$

Under these circumstances an error estimation of f_b results, in which it is shown that error sources cause a total error of

$$f_b \leqslant 0.15 \qquad (4.1.6)$$

Equation (4.1.7) can be satisfied with the smallest effort, when:

$$|E_1 \cdot f_1| = |E_2 \cdot f_2| = |E_3 \cdot f_3|$$

$$E_i \cdot f_i = \frac{f_b}{\sqrt{3}} = 0{,}0866 \qquad (4.1.8)$$

All error factors in equation (4.1.4) must satisfy this condition. For the term which describes the influence of the magnetic field, this boundary, affected by sensitivity factor $E_1=1$, is bound to the condition that the error of the tesla meter and the Hall probe not exceed 8.66%. The measuring instrument producer lists the tolerance as 1%.

The second term of the equation (4.1.4) is described by:

$$E_2 = \frac{1}{2} \cdot \frac{U_L(0)}{U_L(0) - U_L(B)}$$

$$f_2 = \frac{\Delta U_L(0)}{U_L(0)}$$

The error f_2 is dependent upon the amplitude of the lock-in. The measuring program guarantees that the lock-in be driven in a suitable measuring range and that

$$f_2 = 0.01 \qquad (4.1.9)$$

not be exceeded. Sensitivity factor E_2 depends on magnetic field. If $f_2=0.01$, an unbalanced equation can be set for E_2: /68

$$E_2 = \frac{1}{2} \cdot \frac{U_L(0)}{U_L(0) - U_L(B} \leqq 8{,}66 \qquad (4.1.10)$$

The unbalanced equation (4.1.10) can be satisfied only at sufficiently high values of the magnetic flow depth. Inversely, an adjustment specification can be derived with this unbalanced equation.

The following model calculation serves to this end:

$$b = 4000 \text{ cm}^2/\text{Vs}$$
$$U_L(0)/U_L(B) = 1.1$$

Solution of this evaluation equation according to B and integration of the unbalanced equation (4.1.10) results in:

$$B = \frac{1}{b} \cdot \sqrt{\frac{U_L(0) - U_L(B)}{U_L(B)}} \quad (4.1.11a)$$

$$B \geq 0{,}630 \ Vs/m^2 \quad (4.1.11b)$$

The third term

$$E_3 \cdot f_3 = -\frac{1}{2} \cdot \frac{U_L(0)}{U_L(0) - U_L(B)} \cdot \frac{\Delta U_L(B)}{U_L(B)}$$

can be treated analogously to E_2 f_2 and also leads to the unbalanced equation (4.1.10) because of the same sensitivity factor. The different signs of the terms E_2 f_2 and E_3 f_3 has the effect that the error influences caused by the lock-in amplifier are markedly reduced. The error value given in equation (4.1.7) thus represents a high upper limit.

Result: /69

-- The error is less than or equal to 15% because of the measuring instruments and the measuring set-up.

-- Measurements in small magnetic fields (300mT) lead to large mistakes.

-- The general adjustment specification can be given under the condition $E_{2,3} < 8.66$:

$$B \geq 1/4b \quad (4.1.12)$$

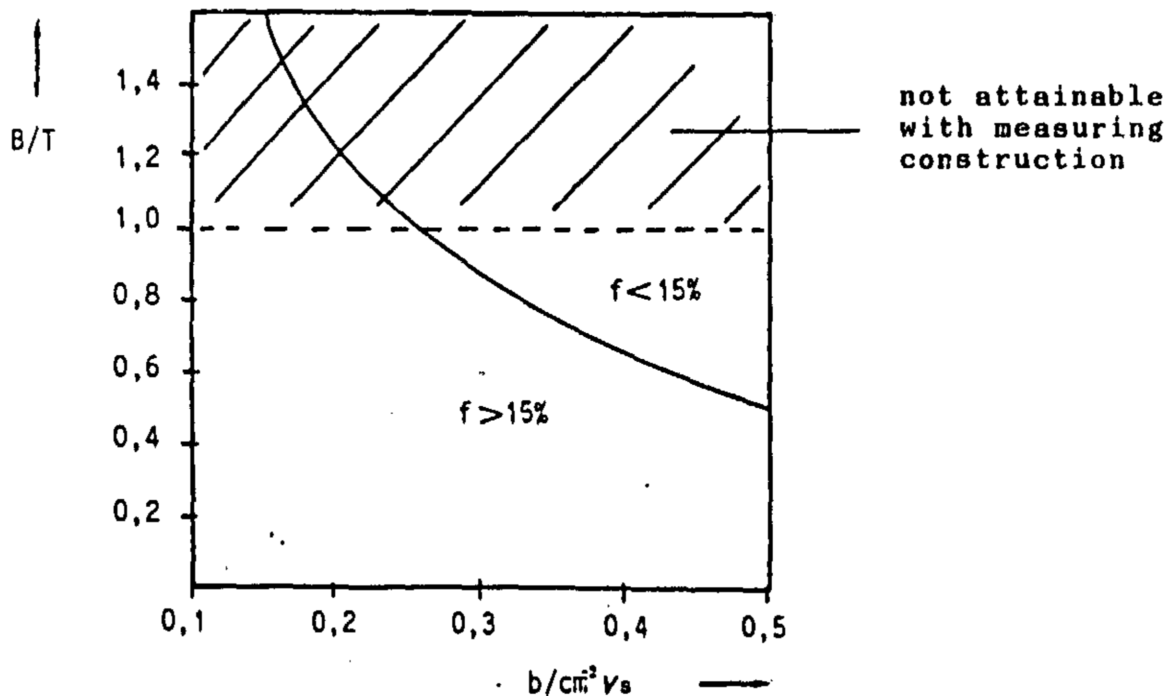

Figure 4.1.1: Adjustment specification for the magnetic field on the basis of acceptable errors and average mobility

The 15% error boundary which can be reached with the present methods is too high to be satisfying. Physical errors would also have to be added to this value. For this reason steps must be taken which reduce error or at least offset errors.

The procedure described in Chapter (2.4.3) lends itself to this goal. /70

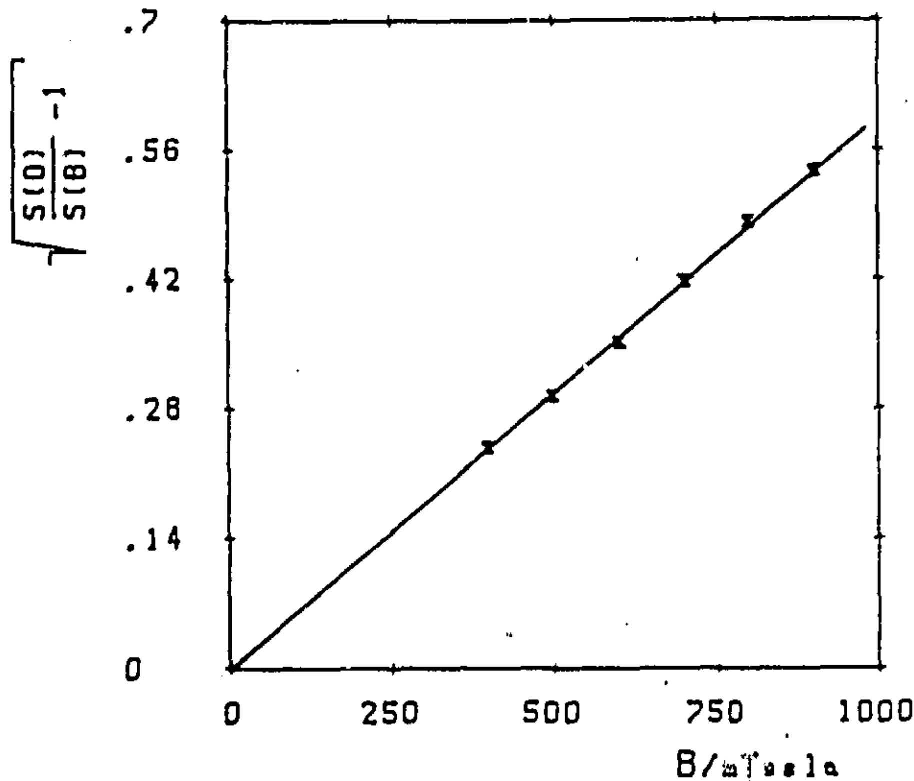

Figure 4.1.2: Error offset by line approximation

Mobility no longer results from a two-point measurement (S(0), S(B)), but rather from a successive measurement

$$S(0),\ S(B_1),\ S(B_2),\ \text{to}\ S(B_n)$$

4.1.3 Statistical procedure /71

In Chapter (4.1.2) error for a single point in Figure (4.1.2) was estimated with the help of the concept of error sensitivity and with measuring instrument precision boundaries. These observations were meaningful and necessary. They indicated sensitive places in the measuring procedure and provided a preliminary adjustment specification for the magnetic field. Nevertheless, a universal error index is not possible since sensitivity factors are especially dependent not only upon the tests but also the working point.

Already at the end of Chapter (4.1.2) a solution was suggested for reducing errors by line offsetting. The evaluation of the data made possible by such a balance becomes optimal with statistical methods:

-- Input data control
-- Statistical error balancing using a linear regression

Physical errors caused by parasitic resistances cannot be determined. If, however, the graph in accordance with Figure (4.1.2) deviates greatly from a straight line, this is indicated by large errors, which result from

-- The drift of the structural element
-- Reaching the physical boundaries of the measuring procedure

With that, the validity control of the evaluation equation recommended in Chapter (2.4.3) is carried out.

4.1.3.1 Control of input data /72

The measuring value reacts to a change in setting dimensions by a transient process in the new stationary end value.

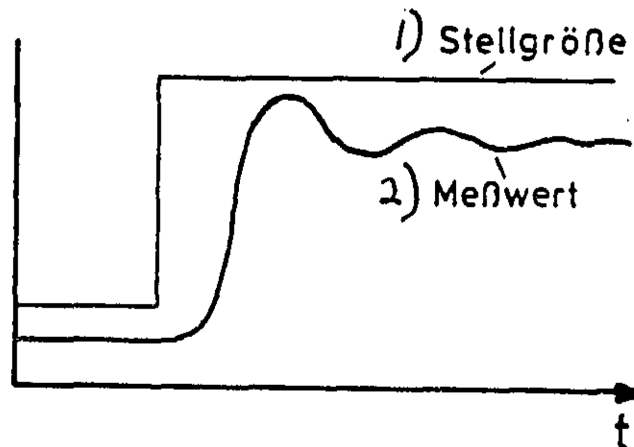

Figure 4.1.3: Transient process of a measuring value after changing the setting dimension
Key: 1) Setting dimension 2) Measuring value

Input data control should

-- Increase the precision of input data by establishing median values from many measuring values
-- Eliminate measurement before a stationary end value has been attained, by controlling the spread of measuring values around the median value

A storage bank is filled with k-measuring values of the same dimension. The measuring values are recorded at intervals T and deposited in the uppermost storage position of the bank. The lowermost (oldest) measuring value drops out.

/73

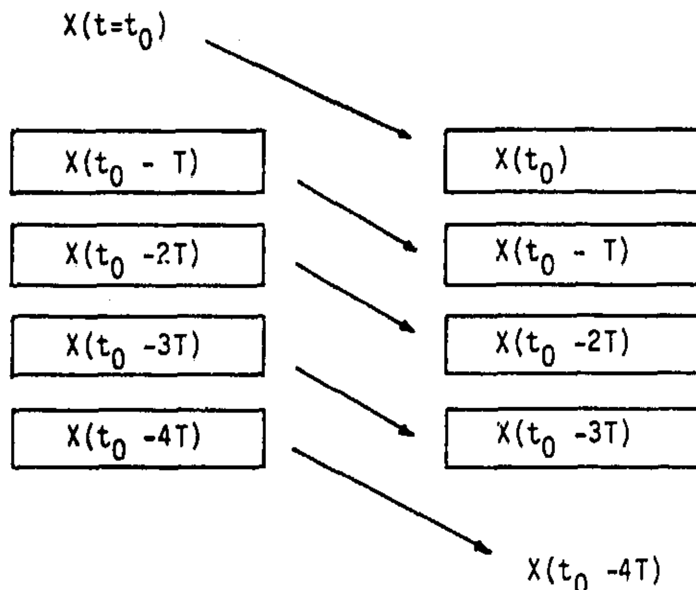

Figure 4.1.4: Storage bank for k=4

The following are formed from measuring values in the bank:

-- The median value
-- The quadratic deviation from the median value, the variance:

$$V = \sum_{i=1}^{k} (\bar{x} - x_i)^2 \qquad (4.1.13)$$

If the variance is too high, then the transient process is not complete and a new measuring value is taken into the pile. This procedure continues until the variance falls beneath a certain level chosen so that the spread around the median value is smaller than the error tolerance of the measuring instrument. Assuming normally distributed measuring values: /74

$$\bar{x} - \frac{\sigma}{\sqrt{k}} \leq U \leq \bar{x} + \frac{\sigma}{\sqrt{k}} \qquad (4.1.14)$$

$\bar{x}$: Median value
u : Statistical threshold value
σ : Standard deviation
U : True value

The equation indicates in which interval around the median value the true value is to be found. According to German regulatory document DIN 55032 error should be estimated so that, with 95% confidence, the true value will not deviate more than

$$\pm \frac{\sigma}{\sqrt{k}} \cdot u$$

from the true value. For this situation /14/:

$$u = 1.96 \qquad (4.1.15)$$

If we now set the following in the first approximation (ideal for $k \to \infty$):

$$\sigma \approx \sqrt{\sum_{i=1}^{k} (\bar{x} - x_i)^2} \qquad (4.1.16)$$

a limit is reached with equations (4.1.14) and (4.1.15):

$$f_x = \frac{\bar{x} - U}{\bar{x}} = \cdot \frac{1{,}96 \cdot \sigma}{\bar{x} \cdot \sqrt{k}} \qquad (4.1.17)$$

Remarks:

The approximation in equation (4.1.16) is relatively rough for sample test numbers k=4 - 6 used in the measuring device. Thus, it is not to be expected that error can be estimated accurately with equation (4.1.17). This procedure primarily provides datacontrol. Formation of the median value causes an error offset in measuring values and, for this reason, substantially improves the precision of the data input.

4.1.3.2 Error offsetting using a linear regression /75

The input data prepared in accordance with the previous chapter allow us to make a diagram on the basis of Figure (4.1.2) The points have the coordinates:

$$\left(B_k \; ; \; \sqrt{\frac{S(0)}{S(B)} - 1} \right)$$

$$(x_k \; ; \; y_k)$$

$k = 1, 2, \ldots, n$

A balancing line can be made using these points in a linear regression.

$$y = a_0 + a_1 \cdot x \qquad (4.1.18)$$

A description of this procedure will be omitted here. Please refer to literature /14/.

Results:

Mobility can be found from the slope of the straight line:

$$a_1 = b \qquad (4.1.19)$$

The procedure produces two error criteria:

1. Zero position error a_0
   Ideally the balancing line goes through origin. If a_0 deviates substantially from 0, then we must assume drift attainment of the measuring procedure validity boundary. /76

2. Coefficient error Δa_1
   With a statistical confidence of 95%, the error determines the error interval around a_1 where the true value of b lies.

Both of these criteria determine the error index in the measuring room expression:

Errors	B/M
%	%

The left-hand value is defined as the percent of intervals around the median value $a_1 = b$:

$$f_b = \frac{\Delta a_1}{a_1} \cdot 100 \qquad (4.1.20)$$

The right-hand value means:

$$f_0 = \frac{a_0}{a_1} \cdot 100 \qquad (4.1.21)$$

It indicates the zero point error in relation to the slope. This somewhat unusual definition became necessary because, unlike the foregoing error criterion, this one lacks a true reference dimension. Taking the absolute value alone is not permissible, since the dimension order of the zero point error is more difficult to recognize.

4.1.4 Drift occarences /77

The linear regression procedure can be optimized primarily by increasing magnetic field settings for every point of the mobility profile. The degree of freedom of approximation increases and error offsetting improves. This possibility does not fail due to pure time expenditure, but rather as a result of the drift in the measuring equipment and the test itself.

The following considerations are aimed at eliminating drifts in the measuring room. The drift of the test cannot be influenced. It is indicated under the foregoing conditions in the error criteria according to equation (4.1.21).

The following table shows which drifts occur in the measuring device. The time period corresponds to seven magnetic field measurements per line approximation.

/78

Parameter	1) Driftzeit s	Drift 2) Ist %	3) Soll %
U_L	245	0,34	0,1
B	35	0,3	1
U_{GS}	245	/	1
U_{DS}	245	/	1
u_{gs}	245	1,0	0,1

Table 4.1.5: Uncorrected drifts in the measuring construction
Key: 1) Drift time 2) Actual % 3) Ideal %

Actual values were attained from measurements in the measuring device. Ideal values are chosen so that drift does not go above the error boundary of the parameter error. The values U_L and u_{gs} exceed permitted drift. It was found that the drift of U_L (initial voltage of the lock-in amplifier) primarily is determined by the drift of u_{gs}. For this reason it is necessary only to make a correction in the alternating voltage of the gate.

Transconductance is calculated from:

$$S = \frac{U_L \cdot S_E}{R_L \cdot u_{gs} \cdot 10V} \quad (4.1.22)$$

Before the correction it was assumed that the value of u_{gs}, set only one time, remains constant for all transconductance calculations during the measuring period. As such, the drift of u_{gs} had a direct and very sensitive influence on the measurement results.

Correction: For every transconductance measurement u_{gs} and u_L were recorded simultaneously. The voltage source continues to exhibit a drift, however, its influence is corrected by technical measuring.

This precaution necessitates additional installation of a second digital multimeter compatible to the IEC-Bus, but it eliminates virtually the entire drift of the measuring device. 79

Parameter	Driftzeit s	Drift Ist %	Drift Soll %
U_L	245	0,033	0,1
B	35	0,3	1
U_{GS}	245	/	1
U_{DS}	245	/	1
u_{gs}	0	/	0,1

Table 4.1.6: Corrected drifts of the measuring device
Key: 1) Drift time 2) Actual % 3) Ideal %

The values in the table are related to seven magnetic field measurements. Since the ideal values are well satisfied, even a considerable increase in magnetic field settings on the side of the measuring device is not critical. The number of magnetic field settings can be governed completely by the type and quality of the test. In the case of tests with minimal mobility, they ought to be as large as the drift allows.

4.2 Technical boundaries of the measuring procedure /80

The measuring technique represented here has two limitations in practical use:

-- Transconductance of the test decreases so much that the entrance sensitivity of the lock-in amplifier is exceded.

-- Charge carrier mobility b is so small that the magnetic transconductance change can no longer be evaluated.

A numerical indication of the limiting values

$$s_S, \ b_S$$

essentially depends on which error boundary is allowed. Since evaluation involves an error indication for every value, the operator may determine these limitations. Here we shall describe the causes and relationships of the limits and, finally, orientation values will be given.

Regarding the transconductance boundary S_S:

At the setting "max output stability", the lock-in amplifier has an initial sensitivity of 100 μV at full force. The smallest permissible value amounts to 20% of the full oscillation.

$$u_L = 20\ \mu V \qquad (4.2.1)$$

From this value the S_S for u_{gs} = 50 mV can be attained:

$$S_S = 400\ \mu S \qquad (4.2.2)$$

If the measuring device was put into operation approximately /81 approximately one to two hours before the measurement, then the lock-in amplifier can be operated at the "normal" setting as well. As a result, initial sensitivity increases by a factor of 100. At this low voltage, however, even the lock-in technique can no longer separate the noise portion with sufficient certainty so that the oscillation swings easily. A lower limitation which can still be evaluated by technical measuring is indicated with:

$$S_S = 20\ \mu S \qquad (4.2.3)$$

<u>Regarding the mobility boundary b_S</u>

Equation (4.1.4) exhibits an additional term

$$f_L = \pm \frac{1}{2} \frac{U_L(0)}{U_L(0) - U_L(B)} \cdot \frac{\Delta U_L}{U_L} \qquad (4.2.4)$$

which describes the error portion of the lock-in amplifier. With help of the equation

$$b = \frac{1}{B} \cdot \sqrt{\frac{U_L(0)}{U_L(B)} - 1} \qquad (4.2.5)$$

a limit b_S can be indicated. The error portion of the lock-in is set at 20%. The measuring instrument tolerance amounts to:

$$\frac{\Delta U_L}{U_L} = 0{,}01$$

With these conditions the following is attained for equation (4.2.4):

$$\frac{U_L(0)}{U_L(0) - U_L(B)} = 40 \qquad (4.2.6)$$

The initial lock-in amplifier voltage decreases by 2.5% in the magnetic field. This small change is the useful information!

/82

$$u_L(0) = 1.025\ u_L(B)$$

With this the following is approximately true for equation (4.2.5):

$$b = b_S \cdot \frac{1}{B} \cdot \sqrt{\frac{1}{40}} \qquad (4.2.7)$$

For a strong magnetic field (B = 900 mT) the lower limit of b is expressed by:

$$b_S = 1760 \text{ cm}^2/\text{Vs} \qquad (4.2.8)$$

Measurements on test III-49 (see Figure (5.1.1) to Figure (5.1.3)) verify this value. The graphic representation of the profile shows, however, that even below this value a mobility profile with a steady course can be obtained. Error offsetting of the linear regression assures that error in the end result lies below occassionally high parameter errors. Since the values spread widely, the necessary statistical certainty of 95% can be maintained only in a relatively large error interval.

These observations can be used to indicate the technical boundaries:

$$S \gg 0.02 \text{ mS}$$

$$b \gg 1760 \text{ cm}^2/\text{Vs}$$

4.3 Setting recommendations for parameter measurements /1*

The parameter settings

$$u_{gs},\ U_{DS},\ B$$

essentially determine measuring precision of the end result. They should be set so that the physical errors and the technical measuring errors maintain the same dimensions. This brings about end results with minimum errors and little effort. Occasionally, both of these error sources cannot be reduced simultaneously, so that the setting recommendations provide a suitable compromise between:

1. u_{gs} minimum
2. U_{DS} minimum
3. B equally distributed
4. B maximum
5. U_L lock-in at full amplitude

*Section 4.3 is included at the very end of the original text, with page numbers as indicated herein.

The compromise between 3. and 4. is found with equation (4.1.11). There the lower limit of B is: $\frac{1}{4 \cdot b}$

b: Estimated value of mobility

This condition is quite astutely described. In practice the following demand proves to be sufficient:

$$B \geq \frac{1}{7 \cdot b}, \qquad (4.3.1)$$

The estimated value of b can be taken from expected test data:

Test	b / cm^2/Vs	B_{min}/mT
Epitaxy	3000	480
Diffusion	2500	580
Ion implantation	4000	360
HETERO	6000	240

/2

Table 4.3.1: Estimated value of mobility in various tests

The remaining value range of B_{min} up to 999 mT is carried out in similar fasion. However, it is not practical to set B-values under 500 mT.

The compromise between 1., 2. and 5. is found when the values of u_{gs} and U_{DS} bring about full amplitude in the lowest range of the lock-in. The following table shows the relationship between transconductance test dimensions as well as S_E (entrance sensitivity of the lock-in amplifier) and u_{gs}.

$$S = \frac{S_E \cdot \frac{U_L}{10V}}{u_{gs} \cdot R_L} = f(u_{gs}, S_E) \ /mS \qquad (4.3.2)$$

u_{gs} mV	Sensitivity S_E		
	10 µV	30 µV	100 µV
30	0.06 - 0.39	0.18 - 1.18	0.61 - 3.94
40	0.05 - 0.30	0.14 - 0.89	0.45 - 2.95
50	0.04 - 0.24	0.11 - 0.71	0.36 - 2.36
60	0.03 - 0.20	0.09 - 0.54	0.30 - 1.97
70	0.03 - 0.17	0.08 - 0.51	0.26 - 1.69
80	0.02 - 0.15	0.07 - 0.44	0.23 - 1.48
90	0.02 - 0.13	0.06 - 0.39	0.20 - 1.31
	$S_u - S_o$		

Table 4.3.2: Calculable transconductance range with dependency of u_{gs} and S_E

Transconductance boundaries are defined so that: /3

$$S = S_u \; : \; U_L = 2 \text{ V}$$
$$S = S_o \; : \; U_L = 13 \text{ V} \qquad (4.3.3)$$

U_L : Exit direct voltage of the lock-in amplifier

With program "B-transconductance measurements" we establish a transconductance profile

$$S = S(U_{GS}, U_{DS})$$

From this profile we seek the measuring series $S(U_{GS}, U_{DS} = \text{const.})$, which at the smallest possible U_{DS} and u_{gs} fits into value range '$S_u - S_o$' of Table (4.3.2).

For partial measurements

-- u_{gs} at the gate contact ($U_{GS} > 0$ V)
-- U_{DS} on the substrate ($U_{GS} \lesssim U_T$)

must be chosen to be very small. Otherwise both voltages should be of the same amplitude (standard value).

5 Results

/83

This chapter contains a selection of measuring results made with the MAGNETO-TRANSCONDUCTANCE-MOBILITY-PROFILING procedure. MESFETS of various technologies were investigated with a wide value range for charge carrier mobility.

The mobility profiles represented are complemented by remarks on the technology of the structural element and the measuring parameters. The selection of measuring results covers the characteristic strengths and weaknesses of the measuring procedure.

5.1 Diffused MESFETs

The active layer is produced by diffusion in semi-isolating GaAs. Diffusion time and temperature are decisive technological data for the concentration of the charge carriers. A look at the comparison between measured results and technology of two diffused MESFETs which were investigated clarifies the influence of technology on the structural element.

a) III-49

The measuring results are represented in Figures (5.1.1) to (5.1.3)

Technical measuring remarks:

/84

Charge carrier mobility lies in the lower boundary range at approximately 1700 cm^2/Vs. Nevertheless, a steady mobility profile was obtained. The b-value of U_{GS} = -1.7 V falls out of the path. In Figure (5.1.2) the triangles represent magnetic field settings for this value and illustrate that apparently drift occurrences lead to this measuring error. The error course of this profile (see Figure 5.1.3), like all the other profiles, agrees well with the expected values. The very high values in the proximity of the boundary layers indicate the boundaries of the measuring procedure. They have their basis in high drift occurrences (boundary layer effects) and lower mobility values.

b) III-78

The measuring results are represented in Figure (5.1.4).

This profile represents a portion of the entire range. Both profiles will be compared following the figures.

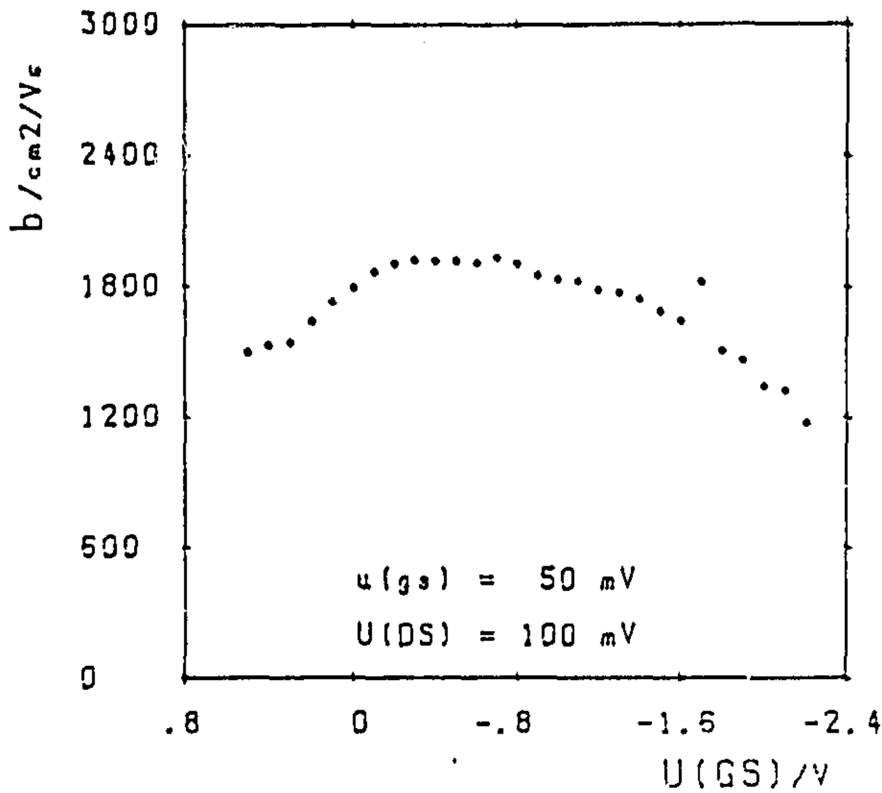

Figure 5.1.1: III-49 Mobility profile

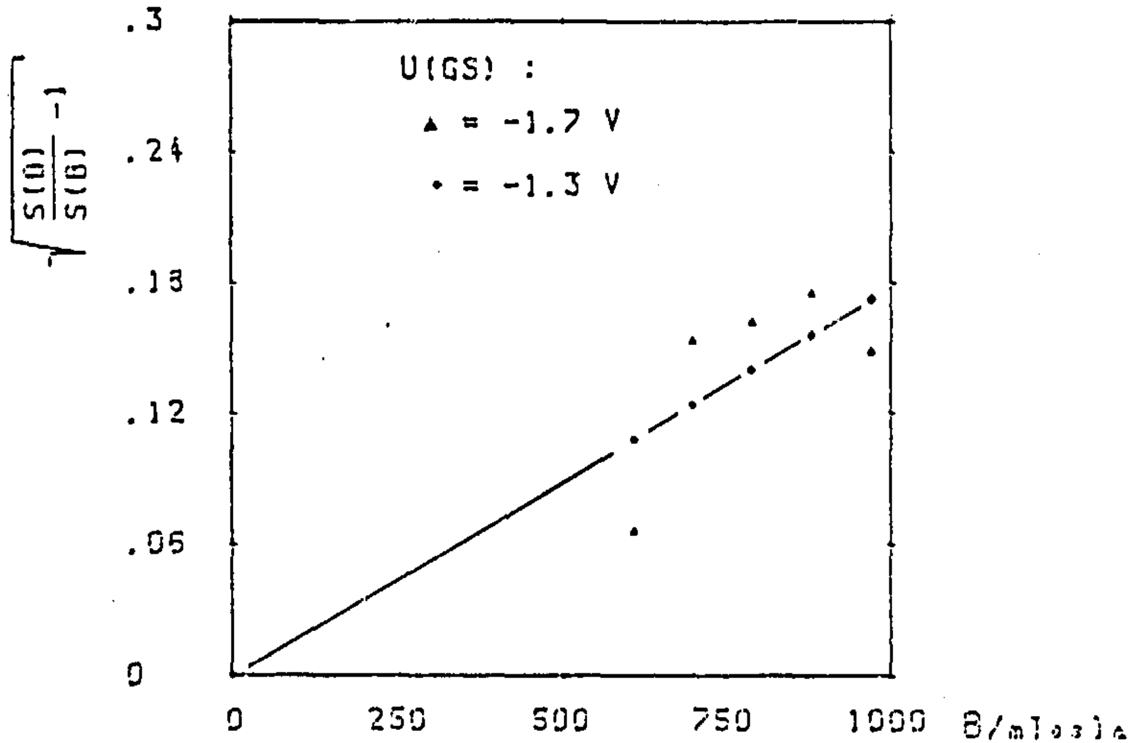

Figure 5.1.2: Line approximation of a good and an erroneous measurement

Test	III-49 10.7
Data input	BIII49 10.7 T
Measuring time	273 minutes
Sensitivity	100 UV
Magnetic field /MT	600 / 970 / 90
Alternating voltage	50MV / 1KHZ
U(DS)	.1 V

U(GS) V	BE CM↑2/VS	ERROR %	B/M %
+0.50	1490	36.3	- 7.5
+0.40	1520	23.5	- 4.9
+0.30	1540	30.9	- 6.4
+0.20	1640	23.8	- 4.9
+0.10	1730	16.7	- 3.4
+0.00	1790	10.7	- 2.2
-0.10	1860	5.9	- 1.1
-0.20	1900	4.7	- .9
-0.30	1920	1.8	- .2
-0.40	1910	3.1	- .5
-0.50	1910	3.2	- .5
-0.60	1900	2.8	- .4
-0.70	1930	1.7	- .1
-0.80	1900	1.5	- .1
-0.90	1850	1.8	- .2
-1.00	1830	1.5	- .0
-1.10	1820	2.3	+ .5
-1.20	1780	2.4	- .4
-1.30	1770	.5	- .0
-1.40	1740	3.3	+ .5
-1.50	1680	1.9	- .2
-1.60	1640	8.2	- 1.6
-1.70	1820	54.9	- 1.4
-1.80	1500	23.3	- 4.8
-1.90	1460	14.5	- 3.0
-2.00	1340	51.9	-10.7
-2.10	1320	6.9	- 1.2
-2.20	1170	69.9	-14.1

Figure 5.1.3: III-49 Tabulated mobility profile

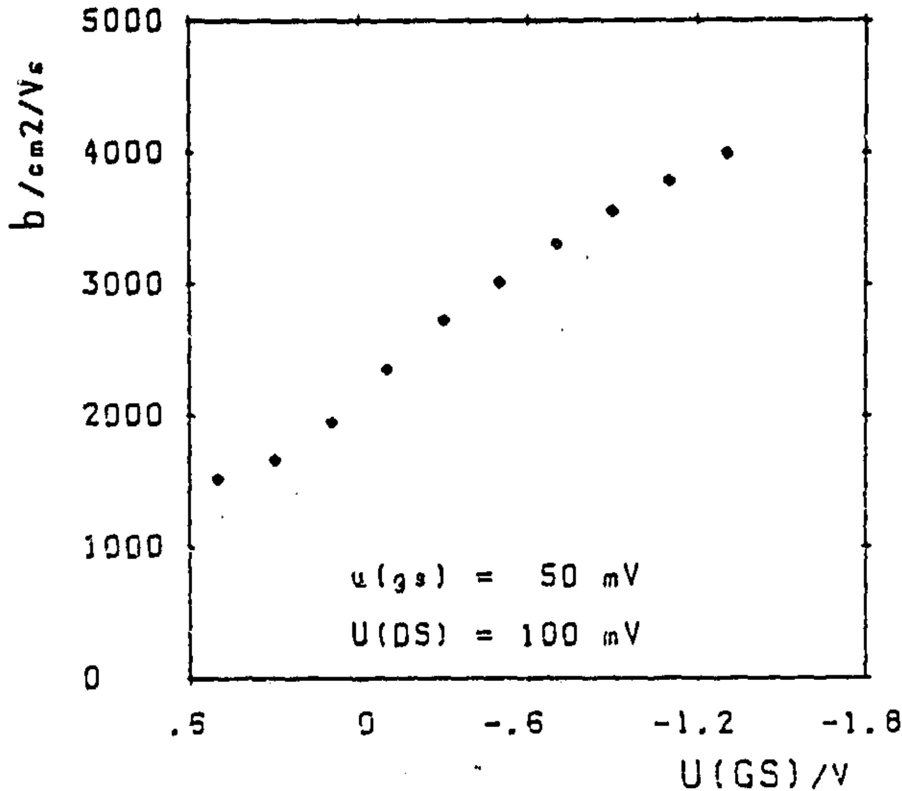

Figure 5.1.4: III-78 Mobility profile

	III-49	III-78
$N_D/10^{18}cm^{-3}$	1,5...2.5	0,6...0,7
T_{Diff}	800 °C	900 °C
t_{Diff}	10 min	36 min
A) Gateabsenkung	B) gering	C) groß
$b_{max}/cm^2/Vs$	1800	4000
f_{max}	15 GHz	21 GHz

Table 5.1.5: Data comparison for two diffused tests
Key: A) Gate decrease B) Small C) Large

The different concentrations can be attributed to diffusion data in connection with the gate decrease. The decline in mobility at the gate contact has different causes in the tests:

III-49: Surface effects
III-78: Steady increase of the disturbance concentration

The data of III-78 are unusual for a diffused MESFET and particularly in relation to its high mobility and high boundary frequency very interesting. According to the instructions of the producer of the structural element, the progress of the charge carrier concentration can be closed upon depletion of the doping material source during layer production.

5.2 Epitaxial-MESFETs

a) I 208-b

This structural element was produced with liquid phase epitaxy (LPE). The measuring results are represented in Figures (5.2.1) and (5.2.2).

Technical measuring remarks:

In spite of the small number of four B-values per line approximation, a very precise mobility profile could be obtained (Figure 5.2.1). A comparison of the error criterion "B/M" with test III-49 clearly shows that the diffused MESFET exhibits a higher drift and that, at nearly identical test mobility, this drift is responsible for the poorer results of the diffused tests. In observing the absolute values of the error criterion "errors in percentage" it should be remembered, that the statistic errors have been evaluated there. A physical error of 5% maximum would have to be added in.

The error boundary increases sharply at I 208-b in the proximity of SI. This allows us to conclude that there are technological difficulties in the boundary surface. /89

b) ALF 1003/1

This MESFET, produced in gas phase epitaxy (VPE), was investigated as an example for an industrial model.

In Chapter (5.1) both of the diffused tests III-49 and III-78 were introduced. At absolute value and course the profile of the I 208-b has a mobility profile similar to that of the III-49. This is also true for tests ALF 1003/1 and III-78. In the tests mentioned last, the decline of mobility at the gate contact can be attributed to the steady increase of charge carrier concentration in both cases. The other tests each exhibit high concentrations, which lead to a decrease of charge carrier mobility.

MOBILITY PROFILE APRIL 28, 1983

TEST	I-208 B 8.5
DATA INPUT	BI208B 28.03 T
MEASURING TIME	86 MINUTES
SENSITIVITY	30 UV
MAGNETIC FIELD /MT	601 / 900 / 100
ALTERNATING VOLTAGE	50MV / 1KHZ
U(DS)	.05 V

U(GS) V	BE CM12/VS	ERROR %	E/M %
+0.50	2270	5.0	- .5
+0.40	2310	2.8	- .3
+0.30	2360	1.0	+ .1
+0.[illegible]0	2360	2.7	+ .0
+0.[illegible]0	2420	1.3	+ .0
+0.00	2420	2.3	- .1
-0.[illegible]	2460	1.8	- .0
-0[illegible]	2490	1.8	- .0
-0[illegible]	2480	3.4	- .3
-0.[illegible]	2480	1.8	+ .0
-0.[illegible]	2450	2.9	- .1
-0.[illegible]	2400	2.1	+ .0
-0.[illegible]	2360	2.8	+ .2
-0.[illegible]	2290	3.5	+ .3
-0.[illegible]	2260	4.8	+ .6
-1.[illegible]	2210	2.8	+ .1
-1.[illegible]	2220	5.4	+ .7
-1.[illegible]	2150	17.3	- 2.1
-1.30	2120	5.0	+ .7
-1.40	2080	22.7	- 2.9
-1.50	2050	18.5	+ 2.2
-1.60	1960	9.9	- .3
-1.70	1900	15.6	- .3
-1.80	1730	21.7	- .2
-1.90	2110	31.1	+ 4.0
-2.00	1720	61.0	- 7.4

Figure 5.2.1: I 208-b Tabular mobility profile

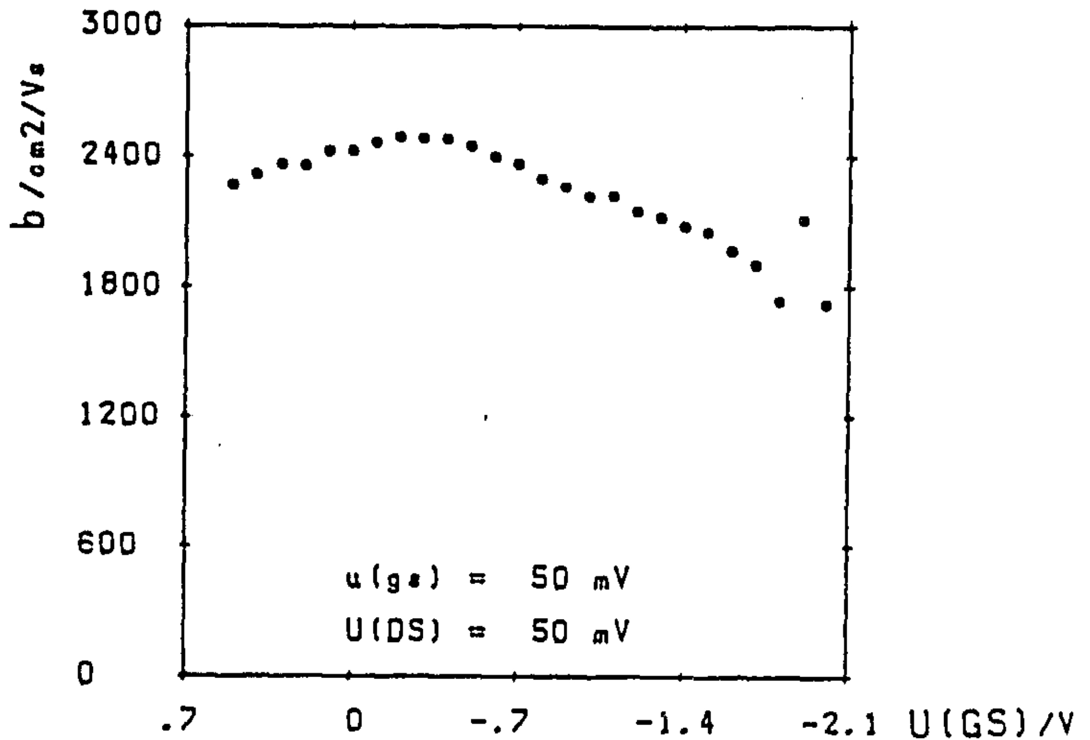

Figure 5.2.2: I 208-b Mobility profile

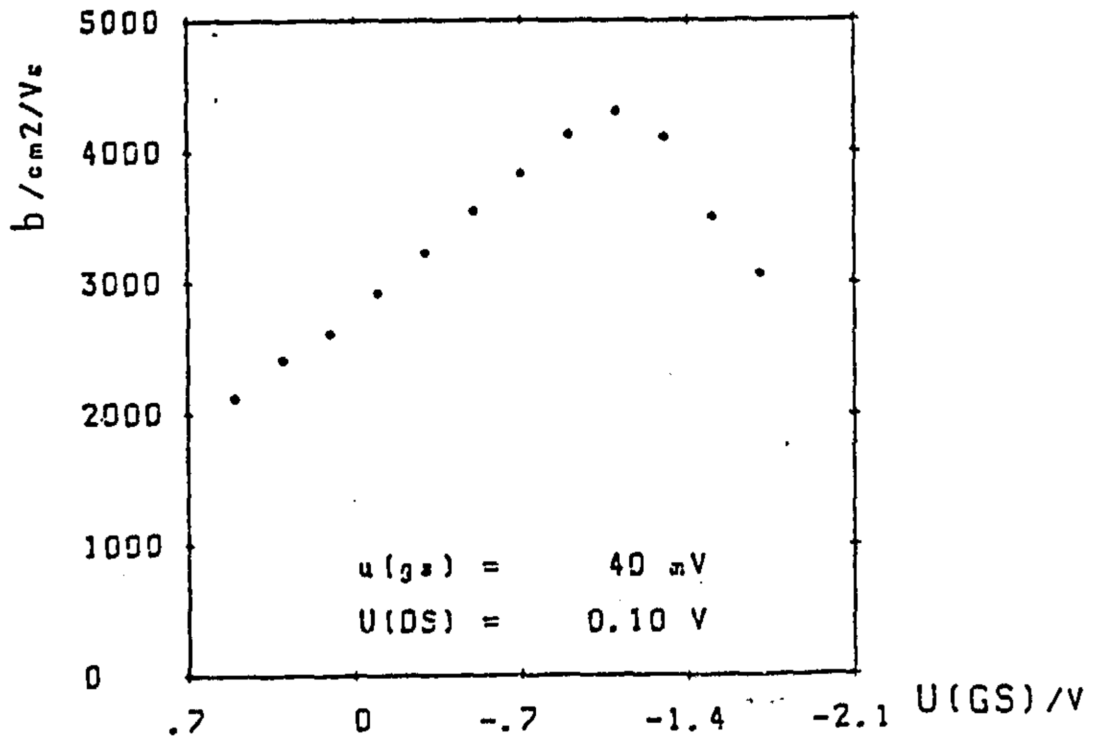

Figure 5.2.3: ALF 10003/1 Mobility profile

5.3 Hetero-structure MESFET

/92

The construction of a hetero-MESFET differs considerably from the homogenously doped structural elements considered thus far. The following figure shows a cross sectional view of the structural element:

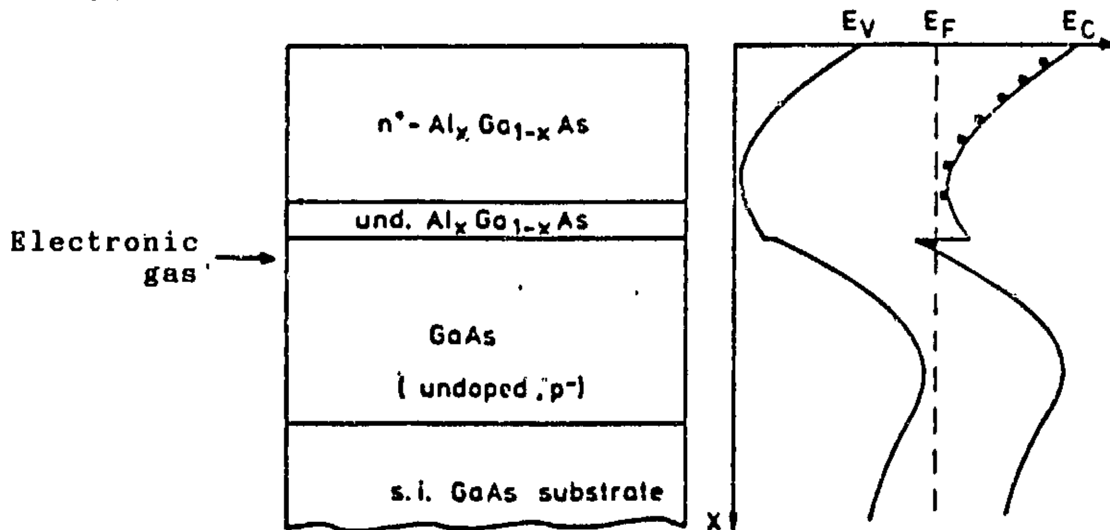

Figure 5.3.1: Structure of a hetero-MESFET

The active layer was produced using molecular ray epitaxy. The literature /17,18,19/ discusses the functioning process of the structural element. The most important characteristic is the formation of a "two-dimensional electronic gas" in the upper boundary layer of the undoped (p^-) GaAs. This produces a very high mobility at simultaneously high charge carrier concentration in a very thin layer. The basis for the high mobility is the very low concentration of ionized disturbance place atoms and the homogenous grid structrue which results from it.

The mobility profile could be determined only insufficiently using integral measuring methods. Thus the Hall measurements yielded a charge carrier mobility of 4500 cm^2/Vs. With the following measurement the actual mobility and its course are recorded for the first time and with it a technical measuring substantiation of the "electronic gas": /93

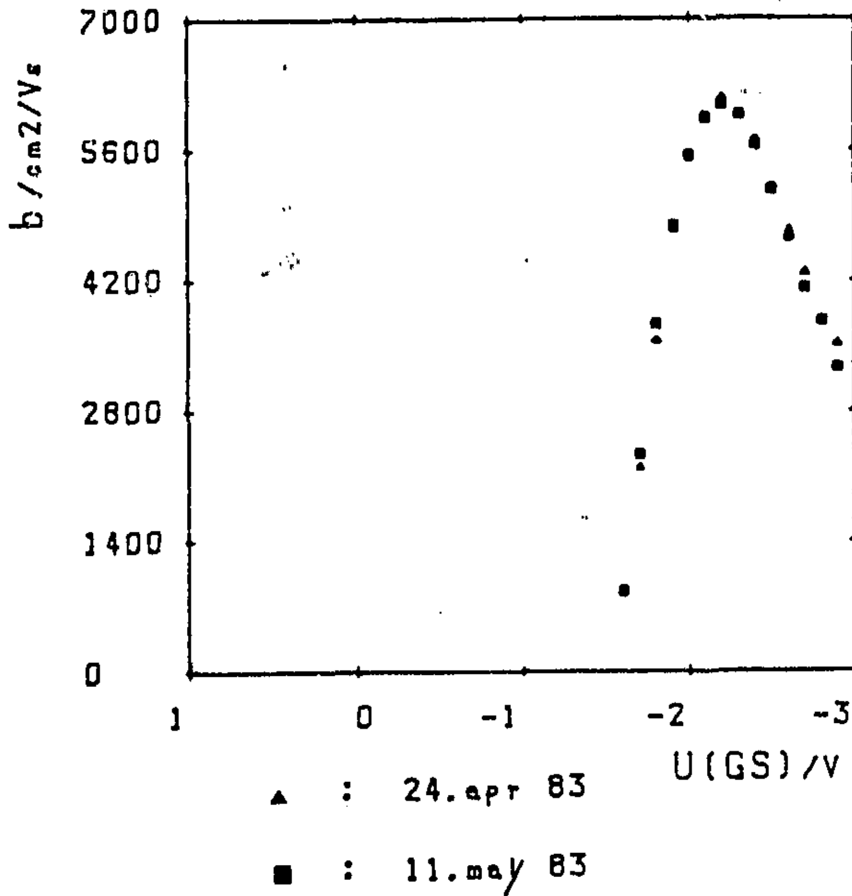

Figure 5.3.2: D-6-9a Mobility profile

The research on this structure has not yet been developed very far. This measuring procedure may contribute a great deal to the further development and understanding of the structural element.

Remarks on the measuring technique /94

In Figure (5.3.1) the profiles of two measurements have been superimposed. The high degree of agreement proves that the measuring procedure can be reproduced successfully. Median deviance between the measurements amounts to 2.3%. Maximum deviance (at SI) amounts to 9%.

6 Summary /95

This measuring procedure enables us to make an actual determination of local mobility in the channel. This procedure is applicable to all current technologies of short-channel-

MESFETs and provides up to $b \approx 1000$ cm^2/Vs useful data. Technological inferences regarding surface disturbances, grid voltage, and quality of the boundary layers are made possible by means of comparison with other parameters in the channel.

Measuring parameters U_{GS} and u_{gs} make it possible to set and cancel depth and layer thickness. This is not possible with any other procedure. As a result of this study, profiles of high precision over the entirety of the channel have been made available. The measuring results for both course and absolute value stand up against results of other works (/1,4,5/). Furthermore, this study provides the first mobility profile of modulation doped hetero-structures measured using this procedure. The results provide a very good look at the functioning processes and quality of this new type of structure.

Other focal points of this study lie in the areas of

-- Measuring room automation.
-- Error control and prevention

Measuring room automation has grown with IEC-Bus compatibility of measuring equipment and instruments. Further progress in this direction is possible only if a lock-in amplifier is developed whose initial sensitivity can be controlled directly by the measuring program. The measuring room can be serviced by a trained lab assitant. /96

The author knows of no publications which deal with error observations of the measuring values. The error criteria developed in this study provide results which agree very closely with theoretically expected procedures. From the observations of statistical and physical errors, a value of

$$f \leq 10\ \%$$

can be given as an error orientation for mobilities over 3000 cm^2/Vs.

Appendix

```
100 rem ###
110 rem ### be = füu(gs)ä      ###
120 rem ###
130 open4,4:open16,16:ch$=chr$(147):printch$:print:print
140 print#16,"b8":sd$="s3v":c$="c99":l$="199":r$="xr":print#4,"s3v0000xr"
150 xz=292.2:xr=438.3:xb=89:rem threshold value for     s=95%
160 print"  data input:     ":print:print
170 print:input" date                        ";da$
180 print:input" test                        ";pn$
190 print:print"     u(gs)        ":print"-----------------"
200 input" starting value      v ";ga:input"  end value         v ";ge
210 input" step width          v ";gs:gf=int((ge-ga)/gs)+2:gn=0
220 ge=ge+.001*gs:if gf<1 then gosub 1030:goto190
230 if (ga-.7)*(ge-.7)<0 or (ga+5.5)*(ge+5.5)<0 then gosub 1090:goto190
240 print:print"     b            ":print"-----------------"
250 input" starting value   mt ";ba:input" end value         mt ";be
260 input" step width       mt ";bs:ba=ba-.01*bs:bf=int((be-ba)/bs)+3
270 if bf<1 then gosub 1030:goto240
280 if gf*bf>300 then gosub 1060:goto190
290 if be>1000 or ba>1000 then gosub 1090:goto240
300 print:input" u(ds)            v ";ud
310 if ud>.3 then gosub 1090:goto 300
320 print:print" alternating voltage ":print"------------------"
330 input" frequency        khz ";f
340 input" amplitude         mv ";a:af$=str$(a)+"mv / "+str$(f)+"khz"
350 print:print" measuring range ":print"--------------"
360 input" sensitivity      uv ";se
370 input" dc-voltmeter      v ";br:br=20000/br
380 input" ac-voltmeter     mv ";ar:ar=20000/ar
390 printch$:print:print:print" magnetic field normalisation ";gosub 1120
400 dim s(gf,bf),a$(152):ww=0:ti$="000000":print"  measurement "
410 for g=ga to ge step gs:g=int(10000*g+.5)/10000:gosub 620:rem r&s spgs source
420 gn=gn+1:bn=0:print:print" u(gs)=";g;" v":print:print
430 for b=be+bs to ba step -bs
440 bn=bn+1
450 if bn>1 then gosub 1300:print" ";b,: rem  b-adjustment
460 if bn=1 then print" b /mt",,"s /ms":print:print"   0",
470 gosub 830:rem k-dmm 10+24
480 if bn>1 or sgn((13-r)*(r-2))=1 then 530
490 print:print:print"  korrektur der lock-in eingangsempfind-     lichkeit"
500 print:print:input" sensitivity     uv ";se
510 print:print" u(gs)=";g;" v":print:print:print"  ";0,
520 goto 470
530 next b
540 print#4,"s3v0000xr":wz=240:gosub 790:if ww=0 then ww=1:bn=0:goto430
550 print#4,"s3v0000xr":print:print:next g
560 m$=ti$:print#16,"b8"
570 print#4,"s3v0000xr":print:print" end of measurement/        evaluation"
580 print:print:print"  store      delete    ":inputme$
590 if me$="s" then gosub 1860:goto610:rem 3000    store
600 if me$<> "1" then 580
610 close6:close4:close16:end
```

```
620 rem ### r&s  voltage source     ###
630 open18,9
640 ua$="ual"+str$(g):ub$="ubl"+str$(ud):print#18,ua$:print#18,ub$
650 wz=60:gosub 790
660 input#18,au$:an=len(au$):if an=24 then an=an-1
670 ua = val(right$(au$,an-3)):ub = val(right$(au$,an-15))
680 if ua<>g or ub <>ud then print "voltage source an"    :gosub750:goto640
690 print#16,"a8"
700 close18:return
710 rem ###   input loop      1   ###
720 getj$:getj$:getj$:getj$:j$="":print:print"                    'j/n'?"
730 get j$: if j$="" then 730
740 print,j$:return
750 rem ###   input loop      2   ###
760 getj$:getj$:getj$:getj$:j$="":print:print"                    'j'?"
770 get j$: if j$<>"j" then 770
780 print,j$:return
790 wt=ti :rem ###    waiting loop    ###
800 if wt+wz > ti then 800
810 return
820 rem ###
830 rem ###measuring value forkeithley multimeter
840 open7,24:open20,10:j=0:wz=300:gosub 790
850 input#20,w$: if st<>0then 850
860 input#7,z$: if st<>0then 860
870 j=j+1:ifw$="over"then print:print"overflow":stop
880 if z$="over"then print:print"overflow":stop
890 r5=r4:r4=r3:r3=r2:r2=r1:r1=val(w$)/br
900 z5=z4:z4=z3:z3=z2:z2=z1:z1=val(z$)/ar:wz=150:gosub 790:if j<6 then 850
910 if j>15 then print:print"   ideal value dmm not convergent   ":j=8:stop
920 r=(r1+r2+r3+r4+r5)/5: rq=(r1-r)ö2+(r2-r)ö2+(r3-r)ö2+(r4-r)ö2+(r5-r)ö2
930 z=(z1+z2+z3+z4+z5)/5: zq=(z1-z)ö2+(z2-z)ö2+(z3-z)ö2+(z4-z)ö2+(z5-z)ö2
940 if zq=0 then 960
950 if z/sqr(zq/4)<xz then 850: rem xz   : 95%wk. for  f< 0.3%
960 if rq=0 then 990
970 ra=sqr(rq/4):rx=r/ra
980 if rx<xr then 850: rem xr: 95%wk. for  f< 0.2%  statement from laplace
990 s(gn,bn)= r/z*se/10:rz=int(1000*s(gn,bn)+.5)/1000
1000 print,rz
1010 if s(gn,bn)>s(gn,1) then print, "drift error" :stop:b=0:gn=gn-1:g=g-gs
1020 close7:close20:return
1030 rem ###  sr  error input  1  ###
1040 print:print"  consult instructions  ":print:wz=60:gosub 790
1050 return
1060 rem ###  sr  error input  2  ###
1070 print:print" amount of data too high     ":print:wz=60:gosub 790
1080 return
1090 rem ###  sr  error input  3  ###
1100 print:print"  measuring range exceeded      ":print:wz=60:gosub 790
1110 return
```

```
1120 rem ### measuring range, b,  d =f(b)      ###
1130 print:print"   maximum value for  b=b(max)":print
1140 mb=1000:if be<95 then mb =100
1150 print:print:print:print"  measuring range tesla water open "
1160 print:print:print:print"           b(max)=";mb;" mtesla     ":gosub 750
1170 d$="0000":print#4,sd$+d$+c$+l$+r$
1180 wz=60:gosub 790
1190 print#16,"b7":gosub 790:print#16,"b7":gosub 790
1200 if d$="0000" then print#16,"a6":gosub 790:print#16,"a6":gosub 790
1210 print#4,sd$+"9999"+c$+l$+r$
1220 printch$:print" talker":print:print" taste inhibit   on  ?" :gosub 750
1230 printch$:print:print:print"  b= ";mb;" mtesla over voltage source"
1240 print:print:print:print" b=";mb;" mtesla ??!":gosub 750
1250 printch$: print:print" taste inhibit  out  ?" :gosub 750
1260 print:print#4,sd$+"0000"+c$+l$+r$
1270 a1=8.6063:a2=1.3937e-3:deffn us(x)=int(a1*x+a2*xö2+.5)
1280 deffn ur(y)=a1+2*a2*y
1290 return
1300 rem ###     b-adjustment       ###
1310 d0=fn us(b)
1320 open12,12:d1=d0
1330 z=0
1340 d$=right$("0000"+str$(d1),4)
1350 aa$=sd$+d$+c$+l$+r$
1360 j=0:print#4,aa$
1370 wz=(1-sgn(z))*240+120:gosub 790
1380 input#12,b$:if st <> 0 then 1380
1390 if len(b$)<6 then 1380
1400 wz=10:gosub 790
1410 er$=right$(b$,4)
1420 e=val(er$)/10*mb/1000
1430 el$=left$(b$,len(b$)-4)
1440 if el$="ee " or el$="6e " then e=e      :goto 1470
1450 if el$="eee" or el$="6ee" then e=-e     :goto 1470
1460 if el$="e  " or el$="6  " then e=e+1000  :goto 1470
1470 if el$="e "  or el$="6 "  then print,,"overload":goto 750
1480 e4=e3:e3=e2:e2=e1:e1=e:j=j+1:if j<5 then 1380
1490 bb=(e1+e2+e3+e4)/4: bq=(e1-bb)ö2+(e2-bb)ö2+(e3-bb)ö2+(e4-bb)ö2
1500 ab=sqr(bq/3):bx=bb/ab
1510 if abs(bb)<.02*mb then 1130
1520 if bx< xb then 1380:rem 95% wkt  for  f<1% (statement from laplace)
1530 rf=abs((b-bb)/b):if rf<.01 and z>0then 1590
1540 z=z+1:ifz>10thenz=5:print:print"  ideal value unattainable    ":stop
1550 dd=int(d1-(bb-b)*fnur((b+bb)/2)+.5)
1560 if dd>9999 then dd=9999
1570 if dd< 1 then dd=5
1580 d1=dd:goto 1340
1590 close12:return
```

```
1600 rem ###    store                    ###
1610 printch$:print:print": load table of contents               ":goto 1840
1620 print:print "opening of document"
1630 print:print"/"are more than 30 blocks free?"      ":gosub 710
1640 if j$="n" then print "new diskette"    stop
1650 print"    from test number and knowledge input new document name"
1660 print:print"name=       >b..............<(15)"
1670 print:input"document name";dn$
1680 if len(dn$)>15 then print"document name longer than 15 characters":goto 1650
1690 n$="@"+ln$+":"+dn$+",s,w":open100,8,10,n$
1700 f2=14:if bf>14 then f2=bf
1710 dim s$(f2)
1720 s$(1)=da$:s$(2)=pn$:s$(3)=str$(ga):s$(4)=str$(ge):s$(5)=str$(gs)
1730 s$(6)=str$(gf):s$(7)=str$(ba+.01*bs):s$(8)=str$(be):s$(9)=str$(bs)
1740 s$(10)=str$(bf):s$(11)=str$(ud):s$(12)=af$:s$(13)=str$(se):s$(14)=m$
1750 for m=1 to 14
1760 print#100,s$(m);chr$(13);
1770 next
1780 for n=1 to gf
1790 for m=1 to bf
1800 s$(m)=str$(s(n,m)):print#100,s$(m);chr$(13);
1810 next m
1820 next n
1830 close 100:return
1840 rem ###      load table of contents              ###
1850 k=0:dim a$(152)
1860 print:print:print:print:print
1870 input"laufwerk 0/1 ";ln$
1880 printch$:print:print:print"    please wait 30 seconds     "
1890 open15,8,15
1900 print#15,"m-e"chr$(212)chr$(237)
1910 open2,8,0,"$"+ln$+":"+"b*"
1920 get#2,a$:get#2,a$
1930 l=1
1940 get#2,a$:get#2,a$
1950 a=0
1960 get#2,a$:if a$<>"" then a =asc(a$)
1970 get#2,a$:if a$<>"" then a =a+256*asc(a$)
1980 a$(l)=str$(a)+""
1990 get#2,a$:a$(l)=a$(l)+a$:if a$<>" " and l<>1 then k=1
2000 get#2,a$:a$(l)=a$(l)+a$
2010 if a$ <> "" then 2000
2020 if k<>1 then l=l+1: goto 1940
2030 close2:close15
2040 rem ###     monitor version of table of contents            ###
2050 print ch$
2060 for n=0 to l
2070 printa$(n)
2080 next
2090 goto 1620
```

```
100 rem ###
110 rem ###   version be-profile        ###
120 rem ###
130 dim s1$(14):ch$=chr$(147)
140 printch$:print:print" read a measurement progression from diskette"
150 print:print:print"choice of measuring progression"
160 print:print" collect table of contents of diskette                ":gosub 1010
170 print:print:print:print:print
180 input" 2 document name";dn$
190 n$=ln$+":"+dn$+",s,r":open 90,8,9,n$
200 printch$:print:print" "load protocol head"
210 for m=1 to 14
220 input#90,s1$(m)
230 next
240 f1=0:print ; "    mobility profile                 ";s1$(1)
250 print" ==================================":print:print
260 print" test                 ";s1$(2):print:print"alternating voltage    ";s1$(12)
270 print:print"  be=f(u(gs))    /cm2v-1s-1":print:print
280 print,"u(ds) = ";s1$(11);" v":print
290 print:print" if measuring progression correct ":gosub 930
300 if j$ ="j" then 330
310 close90:print:print" new measuring progression" :gosub 930:if j$="j" then 160
320 goto 920
330 gf =val(s1$(6)):bf =val(s1$(10)):f1=gf:if bf>gf then f1=bf
340 dim x(f1):dim y(f1):rem for plotter
350 dim s(gf,bf),b(gf,3):t=395/(bf-1)+179:rem approx. threshold value   s=95% bs
360 for gn =1 to gf
370 for bn =1 to bf
380 input#90,sa$:s(gn,bn)=val(sa$):prints(gn,bn)
390 next bn
400 next gn
410 close90
420 for gn =:  ::  gf
430 if s(gn,:  =   then 490
440 for bn =   bf
450 if s(gn,:      then 470
460 s(gn,bn)=   (gn,1)/s(gn,bn)-1)
470 next bn
480 next gn
490 ga=val(s1$    :ge=val(s1$(4)):gs=val(s1$(5)):gn=0
500 ba=val(s1$    :be=val(s1$(8)):bs=val(s1$(9)):bn=0
510 for g=ga t     step gs
520 gn=gn+1:xc     s=0:xs=0:xy=0:bn=1
530 for b=be      step -bs
540 bn=bn+1:xc  c+(b/1000)ö2:xs=xs+b/1000:ys=ys+s(gn,bn):xy=xy+b/1000*s(gn,bn)
550 next b
560 nn=(bf-1)*  :-xsö2:b(gn,1)=((bf-1)*xy-xs*ys)/nn:b(gn,2)=(xq*ys-xs*xy)/nn:bn=:
570 sq=b(gn,2)ö2
580 for b=be to ba step -bs
590 bn=bn+1:sq=sq+(s(gn,bn)-b(gn,2)-b(gn,1)*b/1000)ö2
600 next b
610 sa=sqr(sq/(bf-3))
620 b(gn,3)=t*sa*sqr((bf-1)/nn)/b(gn,1):b(gn,2)=100*b(gn,2)/b(gn,1)
630 next g
640 print:print," table"  ,,"plotter":gosub 950
650 if j$="p" then gosub 1310:goto920
```

```
660 open6,6:fl=0:print#6,,"          mobility profile             ";s1$(1)
670 print#6,,"      ===================================";print#6:print#6
680 print#6,," test                 ";s1$(% ,print#6,, document name        ";dn$
690 z$=s1$(14):z$=str$(val(left$(z$,2))*60+val(mid$(z$,3,2)))+" min"
700 print#6,, "measuring time        ";z$
710 print#6:print#6,,"sensitivity         ";s1$(13);" uv"
720 print#6,, "magnetic field /mt   ";int(ba+.01*bs);"/";be;"/";bs
730 print#6:print#6,; "alternating voltage   ";s1$(12)
740 print#6,,,"u(ds)     ";s1$(11);" v":print#6:print#6
750 print#6:print#6:print#6,,"Ä  u(gs)   Ä     be     Ä error    Ä   b/m  Ä"
760 print#6,,"Ä     v     Ä   cmö2/vs  Ä    %     Ä    %   Ä"
770 q2$="ÄCCCCCCCCCCÄCCCCCCCCCCCCÄCCCCCCCCCÄCCCCCCCCÄ":print#6,,q2$
780 f1$="           a          a           a        a        a"
790 f2$="           a   sz.99  a    99999   a  999.9  a  s99.9 a"
800 close6:open2,6,2:open1,6,1:c$="Ä"+chr$(29)
810 gn=0:print#2,f2$
820 for g=ga to ge step gs
830 gn=gn+1:fl=fl+1
840 print#1,c$;g;c$;int(1000*b(gn,1)+.5)*10;c$;b(gn,3)+.05;c$;b(gn,2)+.05;c$
850 if fl<3 then 870
860 fl=0:print#2,f1$:print#1,c$;c$;c$;c$;c$:print#2,f2$
870 next g
880 close6
890 printch$:print:print" plotter expression  ":gosub 930
900 if j$="j" then gosub 1300:goto 920
910 if j$<> "n" then 890
920 printch$:print:print:print"                 ende":end
930 rem  input loop     1
940 print:print:getj$:getj$:getj$:j$="" :print"                'j/n'"
950 get j$: if j$="" then 950
960 return
970 rem input loop       2
980 print:print:getj$:getj$:getj$:j$="" :print"                'j"
990 get j$: if j$<>"j" then 990
1000 return
1010 rem ###    load table of contents             ###
1020 if yy<>1 then 1050
1030 print:print"  new starting letter          ":gosub 930:if j$="j" then 1070
1040 if yy=1 then 1240
1050 k=0:dima$(152):yy=1
1060 print:print:print:print:print
1070 input" drive     0/1 ";ln$:print:input" input "starting letter of document"  ;ab$
1080 printch$:print:print:print"  please wait 30 seconds     "
1090 open15,8,15
1100 print#15,"m-e"chr$(212)chr$(237)
1110 open2,8,0,"$"+ln$+":"+ab$+"*"
1120 get#2,a$:get#2,a$
1130 l=1
1140 get#2,a$:get#2,a$
1150 a=0
1160 get#2,a$:if a$<>"" then a =asc(a$)
1170 get#2,a$:if a$<>"" then a =a+256*asc(a$).
1180 a$(l)=str$(a)+""
1190 get#2,a$:a$(l)=a$(l)+a$:if a$<>" " and l<>1 then k=1
1200 get#2,a$:a$(l)=a$(l)+a$
1210 if a$ <> "" then 1200
1220 if k<>1 then l=l+1: goto 1140
1230 k=0:close2:close15
1240 rem  table of cont. on monitor
1250 printch$
1260 for n=0 to l
1270 printa$(n)
1280 next
```

```
1300 rem sr ### digi plot ###
1310 print:print:print"    function:":print"    CCCCCCCC":print
1320 input"be=f(u(gs)) -  sqr( )=f(b) -  u&b  ";dw$
1330 if dw$<>"u" and dw$<>"b" and dw$<>"&" then 1320
1340 x1=400:y1=200:y2=1500:rem diagram origin coordinates .
1350 nx=4:ny=5:dx=225:dy=180: rem length and number of axis sections
1360 sd=150:sg=3:sp=sg+1:hb=sp*7: rem sd:abst. d-s / sg:s.gr./hb:s-breite
1370 printch$:print:print" maximum value of be"
1380 input"               cm2/vs   ";um:um=int((um-1)/1000+1)*1000:bm=um/10000
1390 if dw$="b" then 1460
1400 printch$:print:print"      axis scale for       u(gs)":print
1410 print".5  0  -.5  ...-1.5 v  0.5":print" 1  0  -1   ...-3   v  1.0"
1420 input"                       ";uw
1430 print:print:print" axis scale for               ":print
1440 print"  be(max) =";um;"cm2/vs":print"  be(min) = 0;1000;2000...cm2/vs"
1450 input"  be(min)   cm2/vs  ";uu:ud=(um-uu)/ny
1460 printch$:print:print"    diagram drawing       "
1470 input"  enter new data                 ";nd$:if nd$<>"n" and nd$<>"d" then 1460
1480 if nd$="n" then 1520
1490 if dw$="b" then 1510
1500 gosub 1850:if dw$="u" then 1520:rem gosub diagramm be=f(u(gs))ä
1510 gosub 2020:rem diagramm sqr(  )=f(b)
1520 gosub 1800: rem marker choice
1530 if dw$="b" then 1640:rem omission of     be=f(u(gs))-data
1540 close6:open6,5:rem -data  in be =f(u(gs))
1550 for gn =1 to gf
1560 x=dx-int((ga+(gn-1)*gs)*dx/uw+.5):y=int((1e4*b(gn,1)-uu)*dy/ud+.5)
1570 if y=0 then 1610
1580 if x<0 or y<0 then stop:goto1610
1590 if x>nx*dx or y>ny*dy then stop:goto 1610
1600 print#6,"M"+str$(x+x1)+","+str$(y+y2):print#6,mn$.
1610 next gn
1620 print#6,"H":close6:if dw$="u" then1790
1630 print:print:print" sqr(  )=f(b)   data   ":gosub 1800:rem marker  -choice
1640 close6:open6,5:printch$:rem sqr(  )=f(b)
1650 print:print" choice of u(gs)-value       ":print"  ========================"
1660 print:print"u(gs)=  ";ga;" bis  ";gė;"v";spc(20);"step width      ";gs;" v"
1670 print:input"  u(gs)  =ca v";g
1680 gn=int((g-ga)/gs+1+.5):g=(gn-1)*gs+ga:print:print" u(gs)= ";g;"v"
1690 print:print,"  wert   ok":gosub [illegible]:if j$<>"j" then 1650
1700 for bn=2 to bf
1710 x=int((be-(bn-2)*bs)*dx/250+.5):y=int(s(gn,bn)*ny*dy/bm+.5)
1720 if x<0 or y<0 then stop:goto1760
1730 if x> nx*dx or y>ny*dy then stop:goto 1760
1740 if x>0 and y=0 then 1760
1750 print#6,"M"+str$(x+x1)+","+str$(y+y1):print#6,mn$
1760 next bn
1770 print#6,"H":close6
1780 printch$:print:print"  neues u(gs) ":gosub 930:if j$="j" then 1630
1790 close6:return
ready.
```

```
1800 rem ### marker ###
1810 print:print"marke:":print"  punkt      (1)":print" rhombus    (2)"
1820 print"  square    (3)":print"  triangle  (4)":print"double cone(5)"
1830 print"  octagon   (6)":input"                     ";mn$:mn$="N"+mn$
1840 return
1850 close6:open6,5:rem ### be= f(u(gs)) diagramm  ###
1860 uo$="M"+str$(x1)+","+str$(y2):print#6,uo$
1870 ux$="X1,"+str$(dx)+","+str$(nx):uy$="X0,"+str$(dy)+","+str$(ny)
1880 print#6,ux$:print#6,uy$:print#6,uo$:print#6,uy$:print#6,ux$
1890 for n=0 to nx
1900 print#6,"M"+str$(x1+n*dx-hb*(1+abs(sgn(1-n))))+","+str$(y2-sd/2)
1910 print#6,"P"+str$((1-n)*uw)
1920 next n
1930 print#6,"M"+str$(x1+nx*dx-10*hb)+","+str$(y2-sd)
1940 print#6,"S"+str$(sp):print#6,"P U(GS)":print#6,"S"+str$(sg):print#6,"P/V"
1950 for n=0 to ny
1960 print#6,"M"+str$(x1-6*hb)+","+str$(y2+n*dy-sp*3)
1970 print#6,"P"+str$(uu+n*ud)
1980 next n
1990 print#6,"M"+str$(x1-7*hb)+","+str$(y2+ny*dy-10*hb)
2000 print#6,"Q1":print#6,"S"+str$(sp+1):print#6,"Pb":print#6,"S"+str$(sg)
2010 print#6,"P/cm2/Vs":print#6,"Q0":print#6,uo$:close6:return
2020 close6:open6,5:rem ### sqr(    )  = f(b) diagramm  ###
2030 bo$="M"+str$(x1)+","+str$(y1):print#6,bo$
2040 bx$="X1,"+str$(dx)+","+str$(nx):by$="X0,"+str$(dy)+","+str$(ny)
2050 print#6,bx$:print#6,by$:print#6,bo$:print#6,by$:print#6,bx$
2060 for n=0 to nx
2070 print#6,"M"+str$(int(x1+n*dx-.6*hb*len(str$(n*250))))+","+str$(y1-sd/2)
2080 print#6,"P"+str$(n*250)
2090 next n
2100 print#6,"M"+str$(x1+nx*dx-10*hb)+","+str$(y1-sd)
2110 print#6,"S"+str$(sp):print#6,"PB":print#6,"S"+str$(sg):print#6."P/mTesla"
2120 for n=0 to ny
2130 print#6,"M"+str$(x1-6*hb)+","+str$(y1+n*dy-sp*3)
2140 print#6,"P"+str$(n*bm/ny)
2150 next n
2160 rem  root sign
2170 x2=x1-7*hb:x3=int(1.8*hb+.5):x4=int(2*hb+.5)
2180 y3=y1+ny*dy-12*hb:y4=(sg+1)*4
2190 print#6,"M"+str$(x2-x3)+","+str$(y3):print#6,"I0,"+str$(y4)
2200 print#6,"I"+str$(x3)+",0,"+str$(-2*x3)+","+str$(y4)
2210 print#6,"I0,"+str$(9*hb)+","+str$(y4)+",0"
2220 print#6,"M"+str$(x2-x4)+","+str$(y3+4*y4):print#6,"Q1":print#6,"PS(0)"
2230 print#6,"R"+str$(int(hb/2+.5))+",0":print#6,"I0,"+str$(-4*hb)
2240 print#6,"M"+str$(x2)+","+str$(y3+4*y4):print#6,"PS(B)"
2250 print#6,"M"+str$(int(x2-x4/2+.5))+","+str$(y3+4*y4+5*hb):print#6,"P-1"
2260 print#6,"Q0":print#6,bo$:close6:return
```

```
100 rem ###
110 rem ###  s = füu(gs),u(ds)ä  ###
120 rem ###
130 open16,16:ch$=chr$(147):printch$:print:print#16,"b8":f2=0
140 print" constants   ":print:print
150 print:input" date                        ";da$
160 print:input" test                        ";pn$
170 print:rl=1.1:print" load resistance  /ohm ";rl
180 print:print"     u(gs)        ":print"-----------------"
190 input" starting value    /v   ";ga:input"  end value       /v   ";ge
200 input" step width        /v   ";gs:gf=int((ge-ga)/gs)+1
210 if gf<1 then gosub 1230:goto180
220 if(ga-.7)*(ge-.7)<0 or (ge+5.5)*(ga+5.5)<0 then      gosub 1290:goto180
230 print:print"     u(ds)        ":print"-----------------"
240 input" starting value    /v   ";da:input"  end value       /v   ";de
250 input" step width        /v   ";dt:df=int((de-da)/dt)+2
260 if df<1 then gosub 1230:goto230
270 if df>9 then gosub 1260:goto230
280 if gf*df>200 then gosub 1260:goto180
290 if abs(da)>5 or abs(de)>5 then gosub 1290:goto 230
300 print:print"alternating voltage  ":print"-----------------"
310 input" frequency /khz        ";f
320 input" amplitude/mv          ";a
330 print:print"measuring range  ":print"--------------"
340 input" sensitivity/uv        ";se
350 input" voltmeter  dc / v  ";br:br=20000/br
360 input" voltmeter  ac /mv  ";ar:ar=20000/ar
370 dim s(gf,df):dim sd$(gf+1):ge=ge+.001*gs:de=de+.001*dt
380 printch$:print:print:print"      measurement running   "
390 ma=ti:gn=0:dn=0: rem measurement start
400 for d=da to de step dt
410 print:print:print"u(ds)     u(gs)         s":print
420 dn =dn+1:gn=0
430 for g=ga to ge step gs
440 gn =gn+1
450 gosub 800:gosub 1050
460 rem   r$s   ac&dc-dmm
470 next g
480 next d
490 print#16,"b8"
500 ms=(ti-ma)/60:mm=int(ms/60):m$=str$(mm)+" min"+str$(int(ms)-60*mm)+" sec"
510 print:print:print" end of measurement/  expression"  "
520 gn=-1:s1$="CCCCCCCCAC":s2$="CCCCCCCCCCCCCCCCCCCCCCCCCCCCCCCCCCCCCCCC"
530 f2=f2+1:if f2 =2 then print#6:print#6:print#6,,"b= 1000 mt":goto 630
540 open6,6
550 print#6,,"         transconductance measurement         ";da$
560 print#6,,"          ====================":print#6:print#6:print#6
570 print#6,," test                      ";pn$:print#6
580 print#6,," load resistance          ";rl;" ohm"
590 print#6,," alternating voltage      ";a;" mv / ";f;" khz"
600 print#6,,"sensitivity               ";se;" uv"
610 print#6,," measuring time           ";m$
620 print#6:print#6,,"      s=f(u(gs),u(ds)) / ms":print#6:sd$(0)="   u(gs)Ä "
630 f1=3:fm=3:n=-1:print#6,spc(24);"u(ds)"
640 for g=ga-gs to ge step gs
650 gn=gn+1:if gn>0 then sd$(gn)=right$("          "+str$(g)+"  Ä ",10)
660 dn=0
670 for d=da to de step dt
680 dn =dn+1:if f2=2 and gn=0 then 710
690 if gn=0 then sd$(gn)=sd$(gn)+right$("       "+str$(d)+"  ",8):goto710
```

```
700 sd$(gn) = sd$(gn)+right$("           "+str$(s(gn,dn))+"  ",8)
710 next
720 fl=fl+1:fm=fm+1:if fl<5 then 760
730 if fm=5 then s3$=left$(sl$+s2$+s2$,len(sd$(0)))
740 if fm<>5 then s3$=right$("              Ä ",10)
750 fl=1:print#6,s3$
760 print#6,sd$(gn)
770 next
780 if f2=1 then print, magnetic field ;gosub 930:if j$="j" then 380
790 close6:printch$:print:print:print:print,"    ende ":end
800 rem ###
810 rem ### r&s  voltage source     ###
820 rem ###
830 open18,9
840 ua$="ual"+str$(g):ub$="ubl"+str$(d):print#18,ua$:print#18,ub$
850 wz=60:gosub 1020
860 if gn*dn<>1 then 910
870 input#18,r$:rn=len(r$):if rn=24 then rn=rn-1
880 ua=val(right$(r$,rn-3)):ub=val(right$(r$,rn-15))
890 if ua<>g or ub<>d then print"voltage source on    ":gosub 970:goto840
900 print#16,"a8"
910 close18:printd,g;                    :return
920 rem input loop        1
930 getj$:getj$:getj$:getj$:getj$:j$=""
940 print:print"                'j/n'?"
950 get j$: if j$="" then 950
960 return
970 rem input loop        2
980 getj$:getj$:getj$:getj$:getj$:j$=""
990 print:print"                 'j' ?"
1000 get j$: if j$<>"j" then 1000
1010 return
1020 wt=ti :rem waiting loop
1030 if wt+wz > ti then 1030
1040 return
1050 rem ### measuring value of  ac & dc keithley dmm's    ###
1060 open7,24:open20,10:j=0:wz=300:gosub 1020
1070 input#20,w$: if st<>0then 1070
1080 input#7,z$: if st<>0then 1080
1090 j=j+1:ifw$="over"then print:print"overflow":stop
1100 if z$="over"then print:print"overflow":stop
1110 r4=r3:r3=r2:r2=r1:r1=val(w$)/br
1120 z4=z3:z3=z2:z2=z1:z1=val(z$)/ar:wz=150:gosub 1020:if j<5 then 1070
1130 if j>10 then print:print"     ideal value not convergent    ":j=5:stop
1140 r=(r1+r2+r3+r4)/4: rq=(r1-r)ö2+(r2-r)ö2+(r3-r)ö2+(r4-r)ö2
1150 z=(z1+z2+z3+z4)/4: zq=(z1-z)ö2+(z2-z)ö2+(z3-z)ö2+(z4-z)ö2
1160 if zq=0 then 1180
1170 if z/sqr(zq/3)<89 then 1070: rem 89: 95%wk. for  f< 1%
1180 if rq=0 then 1210
1190 ra=sqr(rq/3):rx=r/ra
1200 if rx<89 then 1070: rem 89 : 95%wk. for   f< 1%  (satz von laplace)
1210 s(gn,dn)=int(.00*se*r/rl/z/10+.5)/100:print,s(gn,dn)
1220 close7:close20:return
1230 rem ###  sr error input   1  ###
1240 print:print" consult instructions   ":print:wz=60:gosub 810
1250 return
1260 rem ###  sr error input   2  ###
1270 print:print" amount measuring value too high ":print:wz=60:gosub 810
1280 return
1290 rem ###  sr error input   3  ###
1300 print:print" measuring range exceeded         ":print:wz=60:gosub 810
1310 return
```

REFERENCES

1. Jay, P. R. and R. H. Wallis, "Magneto transconductance mobility measurements of GaAs MESFETs", IEEE Elektron Device Letters Vol. E, No. 10, October 1981.

2. Kuhrt, F. and H. J. Lippmann, "Hallgeneratoren Eigenschaften und Anwedungen", "Characteristics and Applications of Hall Generators", Springer, Berlin, 1981.

3. Jay, P. R. and R. H. Wallis, "Comparison between microwave parameters and magneto tranconductance mobility measurements on submicron GaAs MESFETs", Inst. Phys. Conf. Ser. No. 63, Chapter 9, Paper presented at Int. Symp. GaAs and Related Compounds, Japan, 1981.

4. Sites, J. R. and H. H. Wider, "Magneto resistance mobility profiling of MESFETs channels", IEEE Tran. Electron Devices ED-27, pp. 2277-2281, 1980.

5. Pucel, R. A., and C. F. Krumm "Simple method of measuring drift-mobility profiles in thin semiconductor films", Electronic Letters, May 13, 1976, Vol. 12, No. 10.

6. Tansley, T.L., "AC-profiling by SCHOTTKY gated clover-leaf", J. Phys. E. Scientific Instruments, 1975, 8, pp. 52-54.

7. Muller H., F. H. Eisen, and J. W. Mayer, "Anodic oxidation of GaAs as a technique to evaluate electrical carrier concentration profiles", J. Electrochem. Soc., 1975, 122, pp. 651-655.

8. Jay, P. R., I. Crossley, and M. J. Cardwell, "Mobility profiling of FET structures", Electron. Lett., Vol. 14, 1978, pp. 190-191.

9. Immorlica, A.A., D. R. Decker, and W. A. Hill, "A diagnostic pattern for GaAs FET material development and process monitoring", IEEE Trans. Electron Dev., Vol. ED-27, No. 12, 1980.

10. Jay, P. R., P. Lepoivre, C. Rumelhard, and G. Aperce, "Numerical simulation of the effect of mobility profiles on the microwave response of submicron GaAs MESFETs", Semi-insulating III-V materials, Evian, 1982, Edited by Sherif Makram-Ebeid, Brian Tuck Shiva Publishing Limited.

11. -----------, "Deep levels and electron mobility near the active layer-substrate interface in GaAs-MESFETs".

12. Fukui, H., "Determination of the basic device parameters of a GaAs MESFET", The Bell System Technical JOurnal, Vol. 58, No. 3, March, 1979.

13. Siemans AG, "Bauelemente: Technische Erlauterungen und Kenn daten fur Studierende", "Structural elements: Technical remarks and data for students", Bereich Bauelemente Produktinformation, Munich, 1977.

14. Brauch, Dreyer and Haake, "Mathematik fur Ingenieure", "Mathematics for Engineers", B.G. Teubner Verlag, Stuttgart, 1977, Fifth Edition.

15. Bronstein, and Semendjajew, "Taschenbuch der Mathematik", "Pocketbook for Mathematics", Harri Deutsch Verlag, 1977, 17th Edition.

16. Information sheet ALF 1003/1

17. Dambkes, Heime, Plog, and Weimann, "Influence of contact and properties and dopant concentrations on quasi two-dimensional electron gas field-effect transistor characteristics", Manuscript, "Active microwave semiconductor devices", Maidenhead, 1983.

18. Dambkes, "Field-effect transistor with quasi two-dimensional electron gas channels", Annual Report 1982, Department of HLT, University of Duisburg, 1893.

19. Loreck, Dambkes, Heime, Plog, and Weimann, "Low frequency noise in AlGaAs-GaAs 2-D electron gas devices and its correlation to deep levels", 7th Int. Conf. of Noise in Phys. Systems, Montpellier, 1983.

20. Follinger, O., "Regelungstechnik", "Regulation technology", AEG Telefunken, 1980.